UNIVERSITY OF BERGEN

GEOPHYSICAL INSTITUTE

Master Thesis in Energy

Specialization in Energy Technology

Electrical Power engineering

A comparative study of Doubly Fed Asynchronous and Synchronous Generators in a wind energy perspective

---

By: Rainer Eide

June 03, 2019

Abstract

This master thesis focuses on the analysis of wind generators. It is a comparative study of the Doubly Fed Asynchronous Generator (DFIG) and Synchronous generators (SGs), which also includes knowledge about efficiency, operating conditions, economic perspectives and comparing these factors with one another. Researching relevant literature such as scientific articles, books, and Ph.D. theses are necessary to conclude and discuss which system is better, and which system is best suited for offshore and onshore wind parks. Creating a Simulink program for testing was prioritized. Since there has been a shortage of time, completion of DFIG simulation became more critical. Regarding the SG (more specifically the permanent magnet synchronous generator), choosing a more theoretical approach was deemed better.

Sammendrag

Dette masterstudiet fokuserer på analyse av vindkraft-generatorer. Det er et sammenligningsstudie av den dobbel-matede asynkrongeneratoren og synkrongeneratorer, hvor effektivitet, driftsforhold og økonomiske perspektiv blir vurdert. Forskning av relevant litteratur som vitenskapelige artikler, bøker og doktorgradsavhandlinger har vært nødvendig for å konkludere og diskutere hvilket system som egner seg best, og hvilket system som passer bedre til landbaserte og havbaserte vindparker. Opprettelse av et Simulink-program for testing har blitt mye prioritert. Siden det har vært mangel på tid, ble ferdigstilling av DFIG simuleringen viktigst. For SG (mer spesifikt den Permanent magnetiserte synkrongeneratoren), ble en mer teoretisk tilnærming benyttet.

Preface

The completion of this master thesis marks the end of my five-year education in electrical power engineering. It was made possible by the University of Bergen(UiB) in collaboration with Western Norway University of Applied Sciences(HVL).

I want to thank Lasse Hugo Sivertsen for the advice and guidance along the way. Also, I want to thank Finn Gunnar Nielsen for his help and advice and Midtfjellet Vindpark for allowing a visit to their wind park. A special thanks to Andreas Danmo and Sindre Aarskog for the guided tour in the wind park and showing the interior of their wind turbines. Finally, thanks to classmates, friends, and family for their support during this education.

Contents

List of Figures

List of Tables

Abbreviations

- DFIG —— Doubly fed induction generator
- BDFIG —— Brushless doubly fed induction generator
- BDFIM —— Brushless doubly fed induction machine
- DD PMSG —— Direct driven permanent magnet synchronous generator
- LS —— Low-speed
- MS —— Medium-speed
- HS —— High-speed
- SG —— Synchronous generator
- WT —— Wind turbine
- PM —— Permanent magnet
- PMSG —— Permanent magnet synchronous generator
- PPA —— Power purchase agreement
- AVR —— Automatic voltage regulator
- PSS —— Power System stabiliser
- EMF —— Electromotive force
- WG —— Wind generator
- LVRT —— Low voltage ride through
- SCIG —— Squirrel cage induction generator
- IGBT —— Insulated gate bipolar transistor
- GTO —— Gate turn-OFF thyristor
- AC —— Alternating current
- DC —— Direct current
- HVDC —— High voltage direct current

1 Introduction

The demand for energy is more significant than it has been ever before. An increase in people's standard of living and the population growth profoundly affects the need for more energy sources and production. In the present society, fossil fuel is still one of the most critical energy sources. In time, these resources are at risk of being depleted. There is also a concern regarding the increasing temperature due to the release of CO_2 and other greenhouse gases as a result of using fossil fuel.

More wind energy projects are currently developing, and the need for energy exchange between countries is also increasing. It is contributing to achieving higher power capacity and more climate-friendly energy production. The interconnection of High Voltage Direct Current (HVDC) cables with other countries, allows us to exchange power with other different electrical power systems. If Norway needs to conserve its water reserves, it can import power from The UK or Denmark.

Converting wind into mechanical energy is a known technology, which stretches back many centuries. About 200 years ago, windmills were used to grind grain and raise water for irrigation. They were a common sight at the time. Estimations from that period suggest that Europe had about ten thousand operating windmills at the time. Though in later years the development of windmills for electrical energy production has reached new heights. Between 1990-2005 the average power capacity of wind turbines jumped from 200KW to 2MW. Today wind turbines with a rated capacity of 5-7MW are being tested, and also there are turbines with a rated capacity of 10-20MW being evaluated[25, p.154-166].

The taller and more massive the wind turbine is, the larger the power extraction from the wind is. However, from an economic perspective, bigger does not always mean better. More massive wind turbines are usually in a marine environment where the costs of installing will be higher than onshore. Wind turbines today are mostly being used for electricity production, and are being sold to industrial and residential sectors via the grid[25, p.166].

1.1 Background

Wind energy growth in 2017 has been modest compared to the years 2015 and 2016. Still, it has the third most substantial 12-month period adding 52GW in a global perspective. As a result, the total cumulative capacity has been increased by nearly 11 percent (since the previous year) from 487GW to 539GW. Wind power is now the most economical choice for new power generation in a large and growing market due to its rapidly falling prices, both on- and offshore[22][p.109].

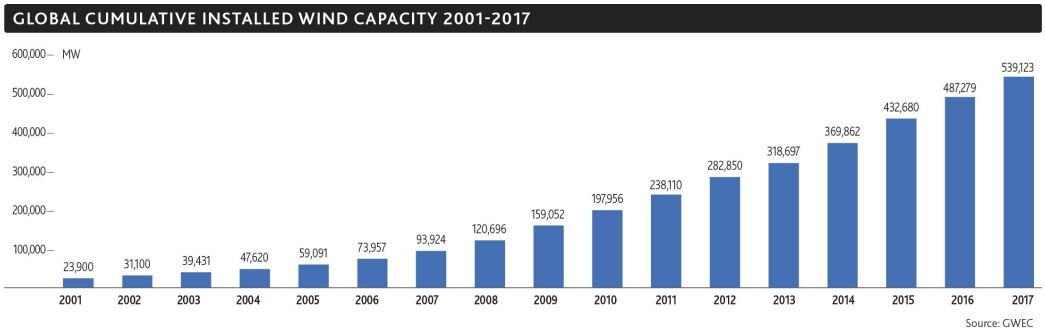

Figure 1: Global cumulative installed wind capacity 2001-2017 [33, p.21]

Norwegian wind energy projects have in the previous year reached new heights. In 2017 a total of 324MW wind power had been installed. Such an expansion of wind energy, allows the country to become a significant wind-powered corporate PPA(Power Purchase Agreement) market in the Nordics. Until recently, most development regarding offshore wind has been at a stand-still, due to expensive technology. As the prices have dropped, the government will now reconsider offshore wind.[33][p.53].

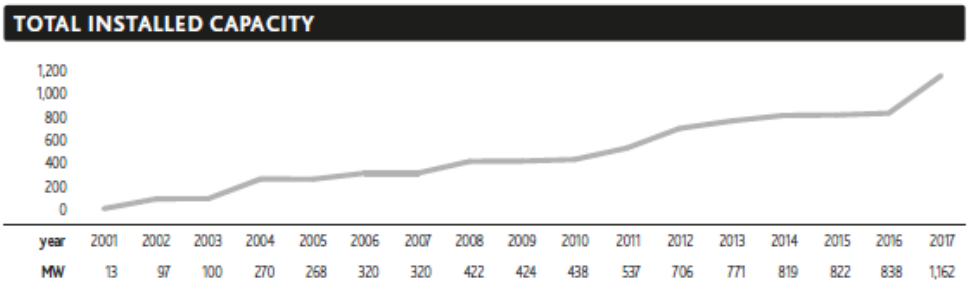

Figure 2: The total capacity of wind energy in Norway [33, p.53]

The first part of the landmark 1,000.8MW Fosen wind farm is expected to be finished in 2018, with the planned connection to the 255MW Roan project. When reaching completion, Fosen wind farm will be Europe's largest onshore wind farm (with its six onshore sites). The Norwegian wind industry is planning to reach about 450MW in 2018. Further the goal is to reach 4GW by 2021 [33, p.53].

1.2 Object of thesis

In this thesis I will focus on the two most commonly used generator configurations and compare their results regarding efficiency, operating conditions and economic perspective. Today the most used generator application is the Doubly Fed Induction Generator (DFIG) and the Synchronous Generator (SG), more specifically the PMSG. This will include gathering information about the generators and their parameters. A Matlab/Simulink model will be created in order to run necessary simulation on the generators.

1.3 Methods

The research presented in this master thesis is of a qualitatively analytic art. Related studies such as Ph.D.'s, articles and books have been essential for developing a table, which compares the properties of both DFIG and PMSG systems.

One of the authors of the book "Doubly Fed Induction Machine Modeling And Control For Wind Energy Generation,"[11] has also published several online guides on how to create Simulink models of DFIG systems. It has contributed to shaping the simulation into what it is now and has been crucial in designing this system. The simulation measures the overall power, current, loss, and efficiency developments at several wind speeds.

In the PMSG system, a more theoretical approach was necessary, which includes related books and studies. Several papers about efficiency, operating conditions, and cost related topics are studied.

How the DFIG operates in a more day-to-day situation, was shown at Midtfjellet Vindpark. The staff answered any questions related to maintenance and operating conditions. Since the work in this thesis is theoretical, a practical demonstration of the DFIG has proven useful in understanding the working principles of this system.

2 Wind aerodynamics

To produce electricity from a wind turbine is to utilize the power of the wind to drive an electrical generator. It is possible by letting kinetic energy of the wind molecules collide with the rotor blades. The result of wind hitting the blades is a reduction in the wind speed in order to increase and maintain the rotational energy of the rotor [17, p.4] [25, p.161].

Kinetic energy in air parcel is given by [25, p.161]:

$$E_{Wind} = \frac{1}{2}mv^2 \tag{1}$$

The mass of the parcel is also equal to the product of air density ρ and volume V [25, p.161]:

$$m = \rho V \tag{2}$$

Which gives:

$$E_{Wind} = \frac{1}{2}\rho V v^2 \tag{3}$$

The volume of the parcel is also equal to its cross-sectional area times the arbitrary length [25, p.161]

$$V = lt \tag{4}$$

Replacing m and V in previous equations, gives us [25, p.161]:

$$E_{Wind} = \frac{1}{2}\rho A v t v^2 \tag{5}$$

Total wind power, passing the area swept by the wind turbine[25, p.161]:

$$P_{Wind} = \frac{E_{Wind}}{t} \tag{6}$$

Can also be expressed as:

$$P_{Wind} = \frac{1}{2}\rho A v^3 \tag{7}$$

The wind power transferred to the rotor is limited to the power factor C_P [17, p.4]:

$$C_P = \frac{P_{Wind\ turbine}}{P_{Wind}} \tag{8}$$

$$P_{Wind\ turbine} = P_{Wind} * C_P = C_P(\lambda, \beta) * \frac{1}{2} * \rho * A * v^3 \tag{9}$$

C_P is, therefore, a function of the tip speed ratio λ and the pitch angle of the wind turbine rotor β [17, p.4].

2.1 Tip-speed ratio

The tip speed ratio is the quotient of the speed of the blade tip (peripheral wind speed) v_{tip}(m/s) to the undisturbed wind speed (upwind free wind speed) [12].

There is also the relation between the tip speed ratio of λ and C_P. Considering both are dimensionless, they are often used to show the performance of any sized wind turbine rotor [17, p.5].

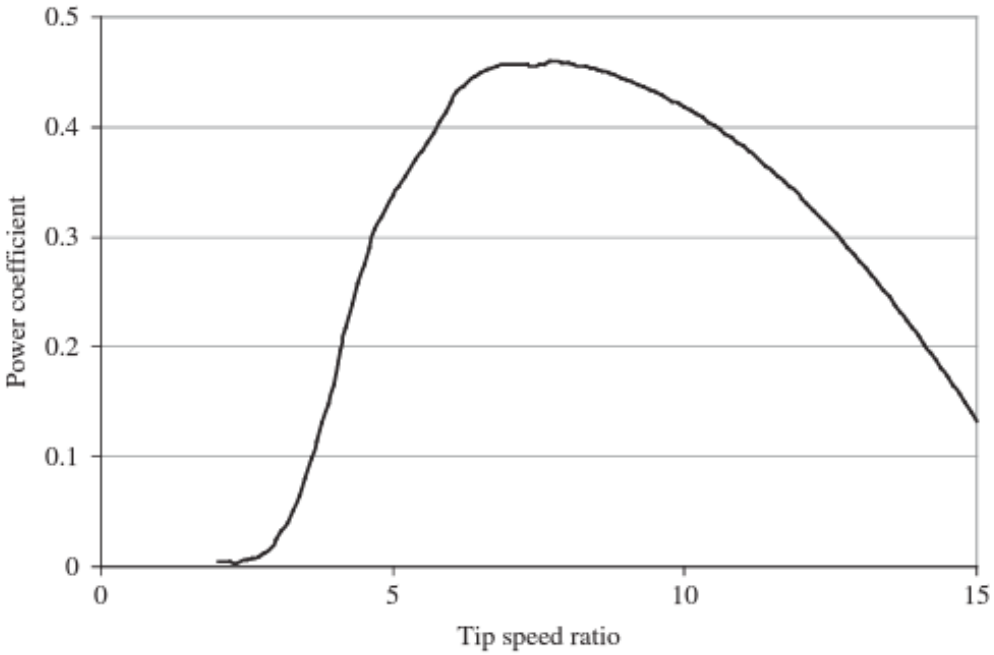

Figure 3: Example of C_P/λ curve [17][p.5]

The formula for tip-speed ratio is as follows [17, p.4]:

$$\lambda = \frac{\omega * R}{v} \tag{10}$$

ω is the rotational speed of the rotor, R is the radius to the tip of the rotor, and v is the upwind free wind speed in meters per second. Figure 3 shows the maximum power coefficient at a single tip-speed ratio. It implicates that the fixed rotational speed wind turbine operates more efficiently at one wind speed, which makes an important argument for the use of wind turbine with variable rotational speed: Max. C_P operation, over a range of wind speeds [17, p.4-5].

2.2 Betz limit and C_P

There are also other limits to the efficiency of a wind turbine. Betz law indicates that the turbine can not absorb the total energy of the wind parcel. Such an absorption would cause the wind to come to a stand-still behind the rotor, which again prevents more wind from passing. Betz limit,

therefore, states that a wind turbine cannot extract more than approximately 59% of the power in an air stream [25, p.162-163].

Another consideration is that a wind turbine, theoretically, would become more efficient with increasing wind speed. In reality, this does not occur since wind turbine systems have a maximum power production limit. In practice, this means that when wind speeds exceed above a given limit, $20\frac{m}{s}$ for example, the efficiency will drop. The conversion from mechanical to electrical energy also contributes to the total efficiency but is usually quite high (about 90%). This results in a total C_P of 30-40% for wind turbines [25, 162-163].

2.3 Fixed-speed topology

Rotor speed, in fixed-speed WT, is determined by the grid frequency. With different wind speeds, the generator speed will usually vary less than 1% (depending on generator size) of nominal speed. With such small variations in the generator speed, one can assume it to be constant.[17, p.6-7].

A typical fixed-speed wind generator is the squirrel-cage configuration. The rotor of this type of generator carries a winding consisting of a series set of bars in the rotor slots which are short-circuited by end-rings at each end of the rotor. When used, it adopts the current pattern and pole distribution of the stator (enabling a basic rotor to be used for machines with differing pole numbers) [32, p.263].

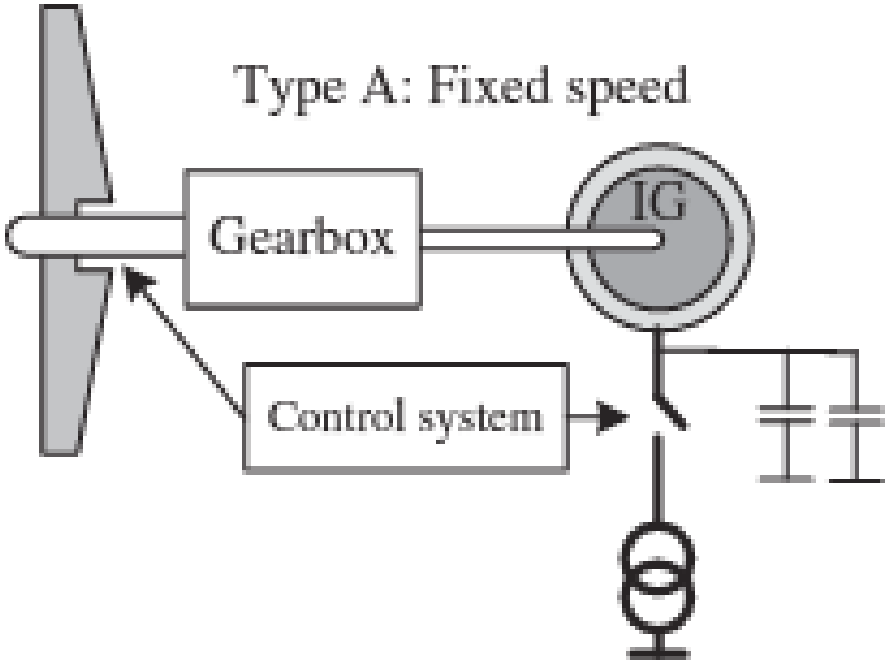

Figure 4: Squirrel-cage generator [17, p.6]

2.4 Variable-speed full converter

There are several alternatives regarding variable speed generators. Asynchronous, conventional synchronous or permanent magnets are the most known generators used in this system. Some of these generators have a gearbox, while others do not.

When power flows through the converter system, the specific characteristics, as well as dynamics of the generator, are isolated from the power grid. With changing wind speed, there will be a change in generator frequency, which also will be isolated from the grid (due to the converter). As a result, the system will be able to run at variable speeds [17, p.7].

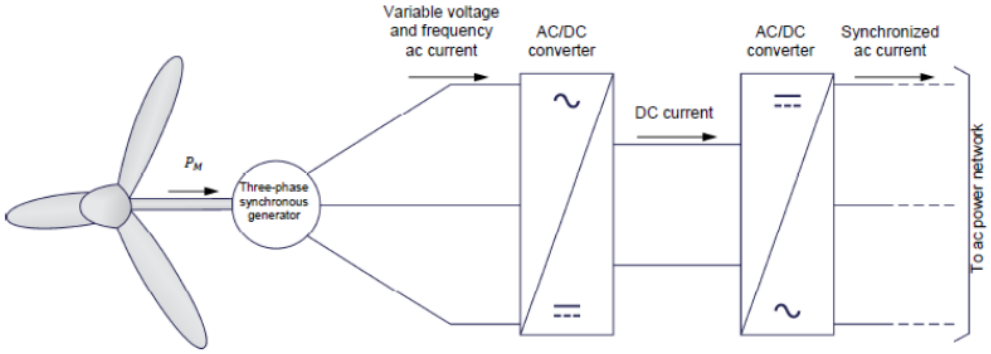

Figure 5: Variable Speed Full Converter System

2.5 Variable-speed partial converter

The partial converter topology is usually associated with the doubly-fed induction generator, where the power converter placement is in the rotor circuit. This configuration allows the generator to operate at variable wind speeds since the changing current and frequency in the rotor circuit is "isolated" from the grid through the converter, shown in Figure 6. The power converter in this case is smaller (About 30%) compared to a full converter system [17, p.7] [32, p.295-300].

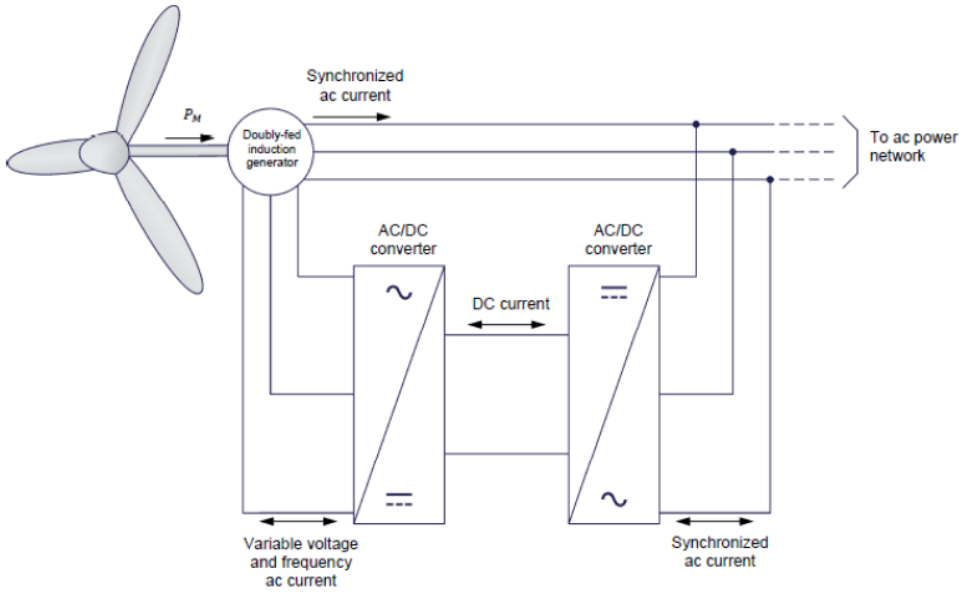

Figure 6: Doubly fed induction generator

3 Synchronous generator

As mentioned in chapter 1.2, the primary purpose of this thesis is to conduct a comparative study of the synchronous generators and the doubly-fed induction generator. In this Chapter, the main goal is to introduce the SG and some of its properties. Among the different SG's that exists today, the permanent magnet synchronous generator holds much promise regarding wind energy technology. Chapter 4 will focus more on the PMSG system.

3.1 Introduction

The Synchronous generator(SG) has been a vital source of converting mechanical energy into electrical energy. Even today, they remain the most substantial energy conversion system in the world. It is used in several power production systems to convert mechanical power from steam turbines, gas turbines, reciprocating engines, hydro turbines, and wind turbines into electricity. The average rating of SG's is between 150KW to 15MW. These machines are common in the industry[32].

Synchronous generators mainly consist of the armature and the field. The armature location is at stator and field at the rotor. The basic principle of SG is that the field windings carries direct current and produces a magnetic field with the rotor and induces an alternating voltage in the armature winding [17, p.73].

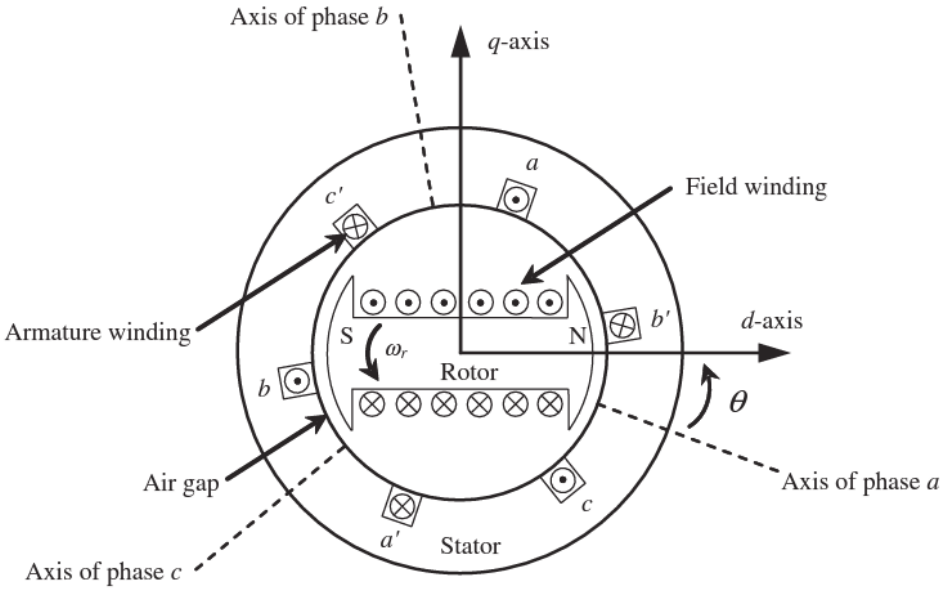

Figure 7: Cross section of 3-phase synchronous machine with two poles[17, p.74]

3.2 Rotor topologies

3.2.1 Salient-pole structure

Usually, the salient pole rotor is in the conventional low-speed generators. It uses a large number of poles to achieve rated frequency. In such a case, the diameter-to-length ratio of the rotor can be made larger. With its low operating speed, this SG configuration is typical in hydraulic turbines. The rotors often have damper windings in the form of copper or brass rods embedded in the pole face. These bars are connected to end rings to form short-circuited windings, to dampen speed oscillations[17, p.73].

Figure 8: Cross-section of salient four-pole synchronous generator[17, p.74]

3.2.2 Cylindrical structure

The cylindrical rotor configuration typically operates in steam and gas turbines due to the high-speed operation. It is made of solid steel forgings, and have typical 2 or 4 poles. The distributed

windings are placed in slots milled in the solid rotor and held in place by steel wedges. Special damper windings are usually not applied since solid steel rotor offers paths for eddy currents, which have comparable effects to those of damper windings. During steady-state conditions, it is the direct current in the field winding that exists in the rotor. Under dynamic conditions, induced eddy currents occur on the rotor surface, slot wall, and in damper windings, which will additionally produce more damping[17, p.73].

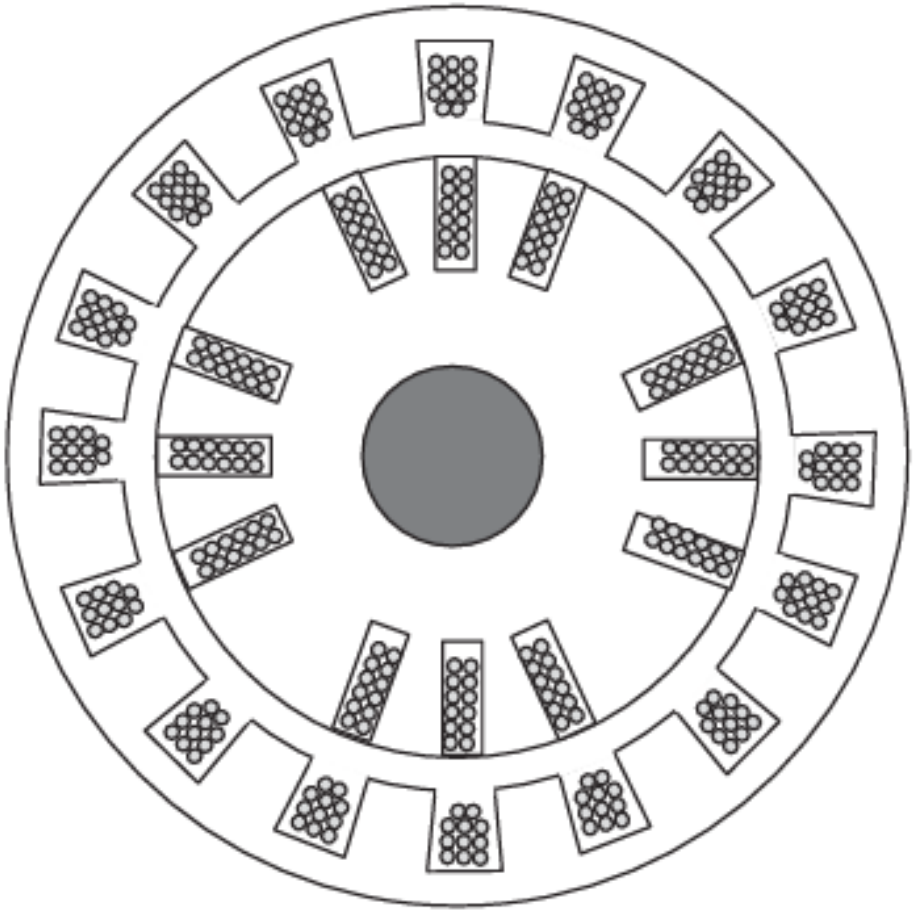

Figure 9: Cross-section of cylindrical four-pole synchronous generator[17, p.74][p.74]

3.3 Poles vs frequency

On a synchronous generator, the number of poles depends on rotational speed and the frequency we want to produce.

$$f = \frac{p * n}{120} \tag{11}$$

Where f is the frequency of induced voltage(Hz), p is the number of poles on the rotor, n is the rotor

speed (r/min)[17, 32].

3.4 Controlling large synchronous generators

In conventional power systems, there will be several different loads and other generators connected through the transmission- and distribution lines. The loads affect the power system, due to their characteristics that may vary in time. In order to keep the power system stable, in case of disturbance (and within limits of voltage and frequency), larger generators are controlled individually and collectively as shown in Figure 10 [17, p.85-86].

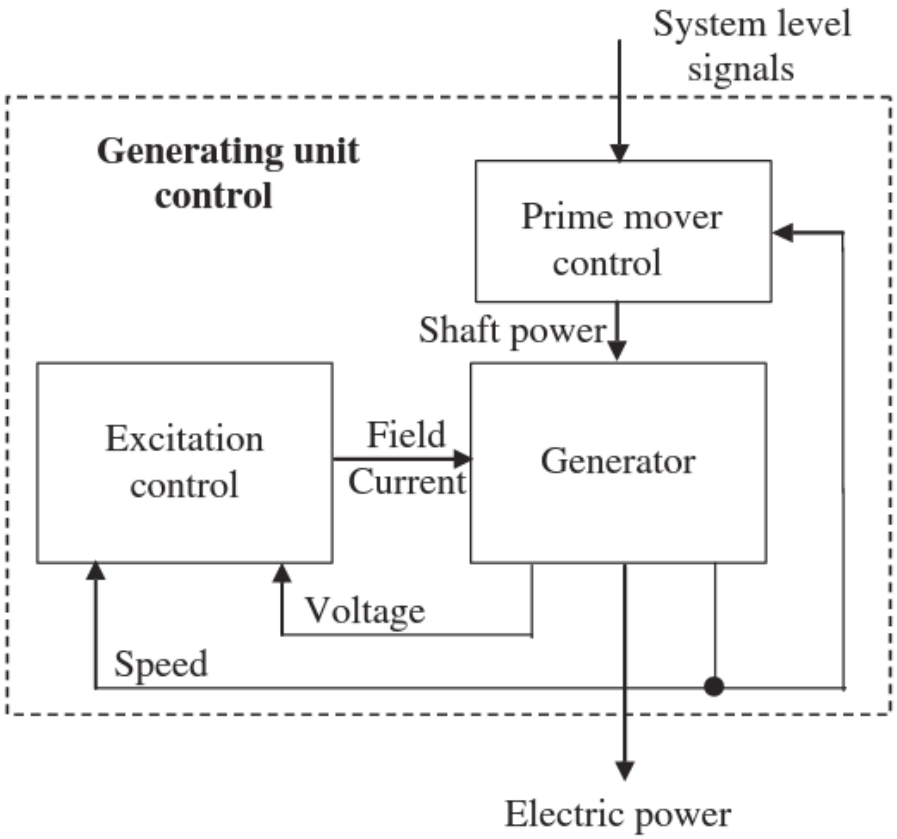

Figure 10: Example of SG control unit[17, p.86]

3.4.1 Excitation

Depending on what kind of load the power system has, the active and reactive power will change. In a high-load condition, the transmission system will absorb reactive power. Thus, the generator must produce more reactive power into the network. In light-load conditions, the power network will have a more capacitive behavior in which the generator has to absorb reactive power. As a response to variations in the reactive power demand, one can adjust its excitation voltage. By

this, the excitation system performs the essential function of automatic voltage regulation as well as performing protective functions required to operate the machine within their capabilities [17, p.86].

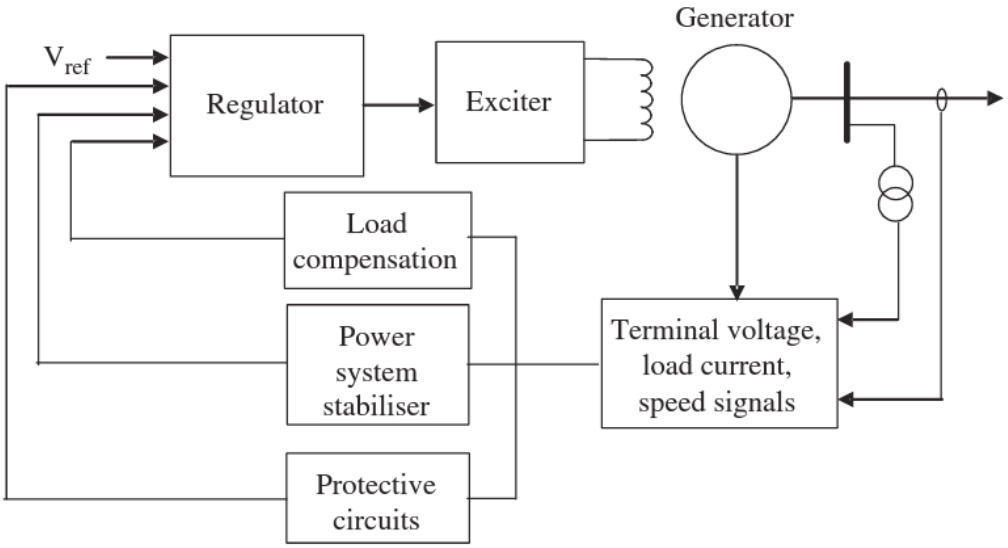

Figure 11: Example of an excitation system

3.4.2 Regulator

The Automatic Voltage Regulator(AVR) maintains the generators stator terminal voltage close to its predefined value. Should the voltage drop due to increased reactive power, the voltage-change will be detected and adjusted. The exciter will receive a signal to produce more excitation voltage. Thus the reactive power is increased, and the terminal voltage is close to initial value [17, p.86].

3.4.3 Exciter

The exciter is mainly used to supply adjustable direct current to the generator field winding. It may be a DC generator on small set sizes. In more massive sets, AC generators are used to supply the field through rectifiers. Static excitation systems is also a possibility, which includes a controlled rectifier typically powered from generator terminals and permits fast response excitation control [17, p.87].

3.4.4 Compensation of load

It is possible to control voltage at a remote point in the network; by building an additional loop to the AVR control. The purpose of the load compensator is to adjust the resistance and reactance that simulates impedance between the generator terminals and the point which the voltage is controlled. The voltage drop is computed and added to the terminal voltage by using the impedance and measured current [17, p.87].

3.4.5 Power system stabiliser

The primary purpose of the PSS is to add damping to the generator rotor oscillations by controlling its excitation. The shaft speed, terminal frequency, and power are the auxiliary stabilizing signals used to control excitation[17, p.87].

3.5 Prime mover control

Allows for the adjustment of the power output so the generators can match the power demand of the network. If the network load should increase, this imposes an increase in torque on the generators, which again causes them to decelerate. The speed reduction is then detected by the governor of each regulating prime mover and are used to increase its power output. The governor drop setting dictates the change in power produced in an individual generator. If the drop is at 4%, this indicates that the regulation suggests that a 4% change in speed results in 100% change in generator output [17, p.87-88].

4 Permanent magnet synchronous generator

This Chapter will explicitly focus on the permanent magnet synchronous generator. The information collected is including scientific articles, books, and Ph.D. theses. The purpose of this Chapter is to study the PMSG, which will be evaluated later on in this thesis.

4.1 An overview of rotors

The basic principle of producing electric energy with the PMSG is no different from other SG's; rotating a magnetic field around a set of windings. When the magnetic field "cuts" across the winding conductors, an EMF is induced. The rotor core (usually composed of iron) and the permanent magnets create the magnetic field. The magnets can be either glued or buried inside the rotor core [17, p.90].

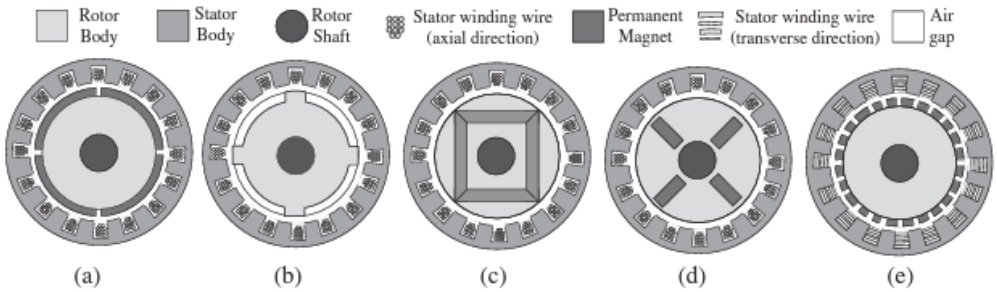

Figure 12: Different types of PMSG[17, p.90]

As Figure 12 indicates, there are several types of PMSG structures. It shows the different cross-section shapes of the rotors depending on what application the PMSG is meant to be used in [17, p.90-91].

- Surface-mounted permanente magnets (a).

  Most used in motor applications[17, p.90-91].

- Inset surface monted permanent magnets (b).

  Most used in motor applications[17, p.90-91].

- Interior permanent magnet (c):

  Used in high-speed operation.

  Rectangular magnets enclose the rotor structure, which gives better mechanical protection against centrifugal forces.

  This type is also used to add reluctance component to the produced torque [17, p.90-91].

- Buried permanent magnet (d):

It promotes flux concentration.

For better performance from ferrite material, the magnet surface area is larger than the rotor surface area.

It is used to add a reluctance component to the produced torque [17, p.90-91].

- Transverse flux permanent magnet (e):

  The topology refers to the direct driven wind energy systems, with low rotational speed and high torque density.

  Single phase configuration of the generator, with ring shaped stator coils.

  There is also an array of surface mounted permanent magnets on the rotor[17, p.90-91].

4.2 Most common topologies of PMSG

The previous chapter explains some of the different rotor cross-sections. Regarding the direction of the flux lines crossing the air gap, there are mostly three topologies which are typical for the PMSG [29, p.25].

4.2.1 Radial flux

This configuration is the most common one for permanent magnet synchronous machines. Also, ship propulsion systems, wind power generation, and robotics use this configuration. The flux lines are in the radial plane, while current flows in the axial direction. The stator of this configuration resembles that of a conventional AC machine. It is easier to manufacture since its a well known and proven technology. The most typical radial flux machine designs are the surface-mounted, inset, and buried magnet configuration. Either of these designs affects the generator weight, performance, and overall cost [29, p.25-27].

The magnets are usually polarized radially, sometimes along the circumference, when being surface-mounted. In order to protect the magnets from centrifugal forces, bandaging of the machine is often necessary. The d-axis and q-axis reactances is almost the same. It makes for a more straightforward rotor construction, compared with other designs [29, p.25-27].

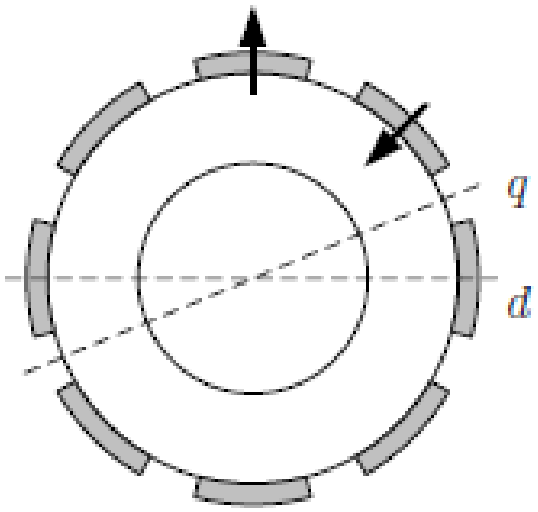

Figure 13: Surface-mounted magnets[29, p.27]

With the inset configuration(Figure 14), magnets are radially polarized and embedded in slots on the rotor surface. There will be a more significant synchronous reactance in the q-axis compared to the d-axis. As a result of more considerable flux leakage, the induced emf by the magnets is usually lower than a surface-mounted rotor design. The rotor is more likely to be lighter, with this design [29, p.25-27].

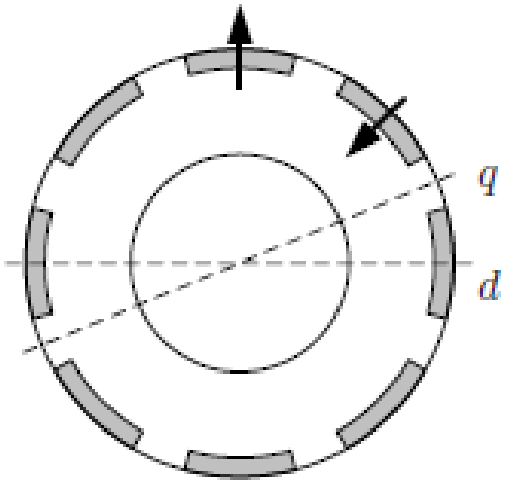

Figure 14: Inset magnets[29, p.27]

Figure 15 shows a cross-section of a buried-rotor magnet configuration. The magnets are here circumferentially magnetized. The q-axis synchronous reactance is here larger than in d-axis. Also, one should carefully choose the thickness of the bridge between magnets. With this configuration,

the use of a non-magnetic shaft is preferable. An advantage to this rotor system is that the air gap flux density can be higher than the remanent flux density of the permanent magnets [29, p.25-27].

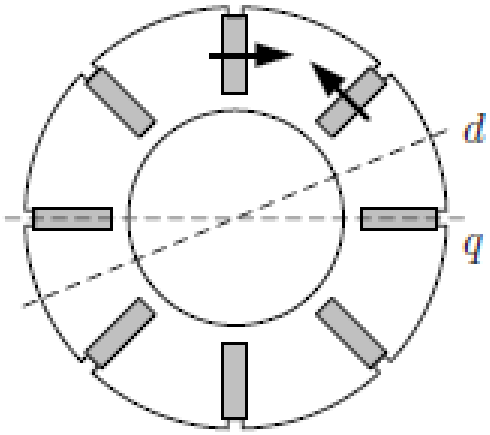

Figure 15: Buried magnets[29, p.27]

4.2.2 Axial flux

With an axial flux machine, the flux lines are crossing the air gap in the axial direction. The windings, however, are arranged radially. The machine has a larger diameter-to-active-length ratio, compared to radial flux machines. The axial flux PMSG consists of two discs, the stator and rotor disc. The rotor disc has permanent magnets, while the stator has armature winding placed in the slots. The machine can have either axially-polarized magnets mounted on its surface, or radially-polarized magnets embedded in its core. It is typically used in traction and servo applications, distributed generation, and propulsion systems [29, p.28].

4.2.3 Transverse flux

A high torque density or multi-pole machines are traits associated with this machine topology. Typical areas for the transverse flux machine are free-piston generators for hybrid vehicles, wind energy, and ship propulsion systems. The flux lines lie in the perpendicular or transversal plane to the direction of movement and that of current flow [29, p.28-29].

The advantage of the transverse flux machine is its ability to attain a high torque density. By increasing the number of poles, for given dimensions and current loading, this is possible. However, when designing this machine, the mechanical rigidity should be checked since the pole pitch has a lower bound [29, p.28-29].

The transverse flux machine also allows for the current and magnetic load to be set almost independently. The width of the machine determines the current loading while the pole length set the magnetic loading. It affects the construction of the machine since the armature winding, and the magnetic circuit does not compete for the same space [29, p.28-29].

However, this machine has a poor power factor because of high flux leakage. There is a solution to this; to increase the pole width. However, this happens at the cost of relinquished high torque density. When designing a transverse flux machine, the trade-off between performance and utilization of active materials is evaluated to find an optimal solution. In case of failure, the short-circuit current would be limited due to the large leakage reactance [29, p.28-29].

Transverse flux machine also requires a complicated mechanical structure of the magnetic circuit. The magnetic circuit consists of many separate small-sized components, which results in a relatively weak construction and more complex manufacturing[29, p.28-29].

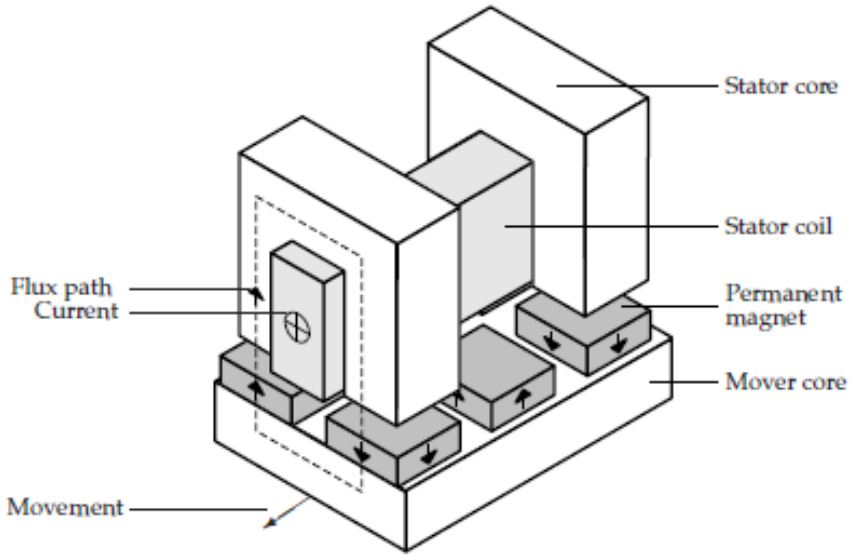

Figure 16: Single-phase transverse flux topology with PM excitation[29, p.29]

4.3 Difference in PM's vs electrically-excited generators

There are two ways a synchronous generator can obtain excitation. The methods are current-carrying windings or permanent magnets. Wound-rotor SG's can adjust its excitation current, resulting in control of its output voltage independent of load current. However, they are also heavier and usually bulkier than the PM generators. In electrically-excited generators, the rotor losses are higher. The permanent magnets also cause some losses due to the circulation of eddy currents in the PM volume. However, the losses are lower compared to the electrically-excited generator[17, p.91-92].

4.4 Equivalent circuit

Equivalent circuit shows the PMSG in d-q reference frame.

Voltage equations for the equivalent circuits are [21]:

$$\frac{d}{dt}i_d = \frac{1}{L_d}v_d - \frac{R}{L_d}i_d + \frac{L_q}{L_d}p\omega_r i_q \tag{12}$$

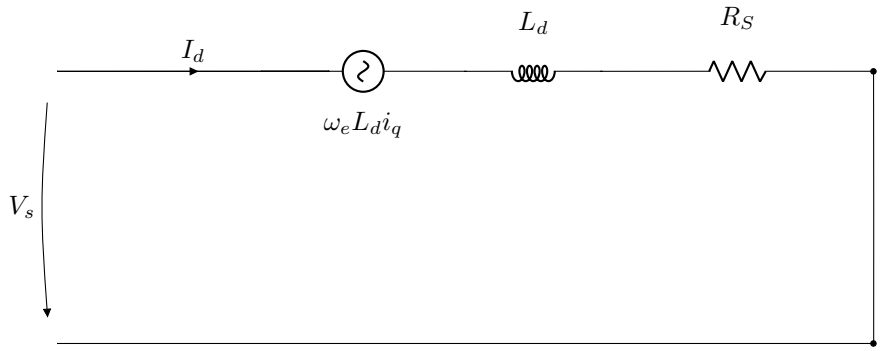

Figure 17: d-axis equivalent circuit [21, p.6]

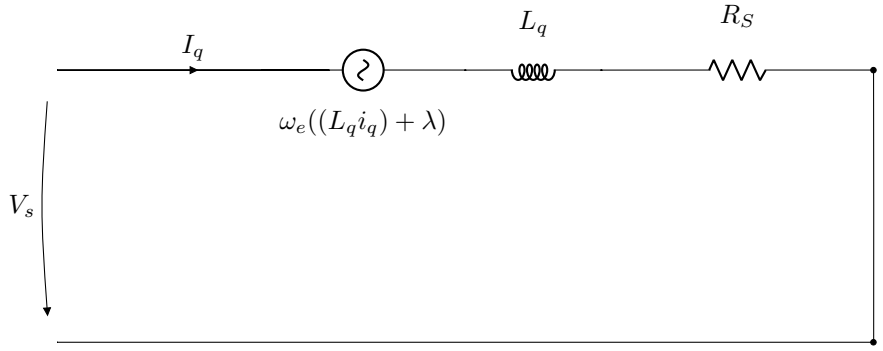

Figure 18: q-axis equivalent circuit [21, p.6]

$$\frac{d}{dt}i_q = \frac{1}{L_q}v_q - \frac{R}{L_q}i_q + \frac{L_d}{L_q}p\omega_r i_d - \frac{\lambda p\omega_r}{L_q} \tag{13}$$

Equation for electromagnetic torque is given by [21]:

$$T_e = 1.5p[\lambda i_q + (L_d - L_q)i_d i_q] \tag{14}$$

Symbol	***Explanation***
L_q	q axis inductance
L_d	d axis inductance
R_s	Resistance of stator windings
i_q	q axis current
i_d	d axis current
v_q	q axis voltage
v_d	d axis voltage
ω_r	angular velocity of the rotor
λ	Amplitude of flux iduced
p	Number of poles

Table 1: Notations to equivalent circuit[21, p.6]

4.5 Some losses in PMSG

In the permanent magnet synchronous generator, both the copper and magnetic losses are the largest sources of losses. The magnitude of these two depends if the generator is in a no-load or loaded condition. At no-load, the magnetic losses have the largest share of losses. At loaded condition, the copper losses are more significant (Depends on generator design). This Chapter mentions the mechanical, gearbox, copper, and converter losses in the PMSG wind energy system[30, p.16].

4.5.1 Mechanical losses

Either manufacturing tools or empirical formulas do the calculation of bearing losses. Here is an example of an empirical formula used for smaller machines [30, p.18]:

$P_b = 0.5 * C_{fb} * F * d_b * \Omega[W]$

- C_{fb} is the constant coefficient of friction bearing
- F is the equivalent dynamic bearing load[kN]
  Can be calculated from radial and axial components of bearing load.
- d_b is bore diameter [mm]
- Ω is the angular frequency of the shaft supported by the bearing [rad/s]

A more straightforward way of expressing bearing loss[31, p.37]:

$W_b = K_B * \omega_m[W]$

- K_B includes weight of rotor, diameter of axis and rotational speed of axis

The friction loss that occurs between air and rotor is called windage loss[31, p.37]:

$W_w = K_w * (\omega_m)^2[W]$

- K_w is determined by rotor shape, lenght and rotational speed.

Since the rotational speed of a PMSG is usually very low, both the windage and bearing losses are small[31, p.37].

4.5.2 Gearbox losses

Gearboxes are typically in use for medium or high-speed PMSG systems. ABB has created some solutions for this:

Fully integrated gearbox (MS PMSG):

- Both generator and gearbox share the same shaft, frame, and bearings. Manufacturers of generator and gear must together develop a solution for this [7].

Semi-integrated gearbox (MS PMSG):

- A two-stage gear integrated with the generator via a flange connection [7].

Non-integrated gearbox (MS and HS PMSG):

- "Generator is a seperate unit, mounted independently of the gearbox, representing a similar system to those used in high speed drivetrains" [7]

However, losses from gearbox only apply if they are in the medium or high-speed range. In DD PMSG systems the gearbox losses are neglected.

Gearbox losses can be calculated similar to that of a DFIG system, see Chapter 5.4.1.

4.5.3 Copper loss

The copper loss for a three-phase generator can be calculated in the following way[30, p.22]:

$P_{cu} = 3 * R_{ph} * (I_{ph})^2$

- R_{ph} is the DC resistance of each phase
- I_{ph} is phase current

4.5.4 Stray load loss

The stray load loss is somewhat complicated to calculate accurately. It occurs in the generator at a loaded condition. This type of loss consist of eddy current losses in conductors, iron core and adjoining metallic parts generated by the flux leakage. An approximate expression of this is [31, p.37]:

$W_s = 0.005 * \frac{P^2}{P_n}(W)$

4.5.5 Converter losses

Many articles and theses calculate the converter losses more accurately. This thesis will not go in any detailed power calculation regarding converters. Most of the power converter systems today have an efficiency of about 97-99%. In this thesis, an efficiency of 97% was chosen, according to ABB's datasheets [1]:

$P_{ConverterLoss} = 0.03 * P_{in}[W]$

5 Doubly fed induction generator

This Chapter introduces the doubly-fed induction generator. Chapter 5.4 also discusses the brushless doubly-fed induction generator. However, the DFIG proved more suitable for continued research and analysis. Chapter 5.5.2 summarizes some reasons for this. The information in this Chapter is meant to give an overall evaluation for later comparison.

5.1 About the DFIG system

A doubly-fed induction generator is a machine where the stator is directly connected to the grid, while the rotor winding is, through slip-rings, connected to the converter. There are some DFIG configurations which also makes it possible to exclude the slip rings and carbon brushes. As a variable speed wind generator, it has become quite popular. The reason for this is the reduced cost and size of the power conversion system. Also, converter losses are smaller compared to a fully rated converter system. It only has to handle a fraction of about 20-30% of the total power. It results in a reduced system cost[27, p.13].

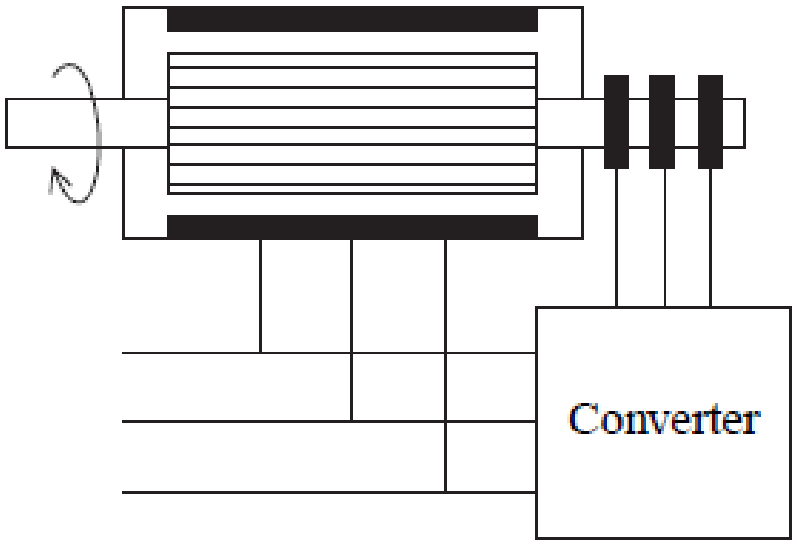

Figure 19: DFIG principle of using a back-to-back converter [27, p.13]

Figure 20 shows how a back-to-back converter can be used at the rotor side of the DFIG. It consists of two converters, one ac-dc at rotor side (or generator side) and one dc-ac at grid side. A capacitor is placed between them to eliminate/reduce variations in the voltage (ripple) in the dc-link. Either torque or speed is possible to control at generator side of the converter, as well as the power factor at stator terminals. Main goal of the grid-side converter is to keep dc-link voltage constant [27, p.13].

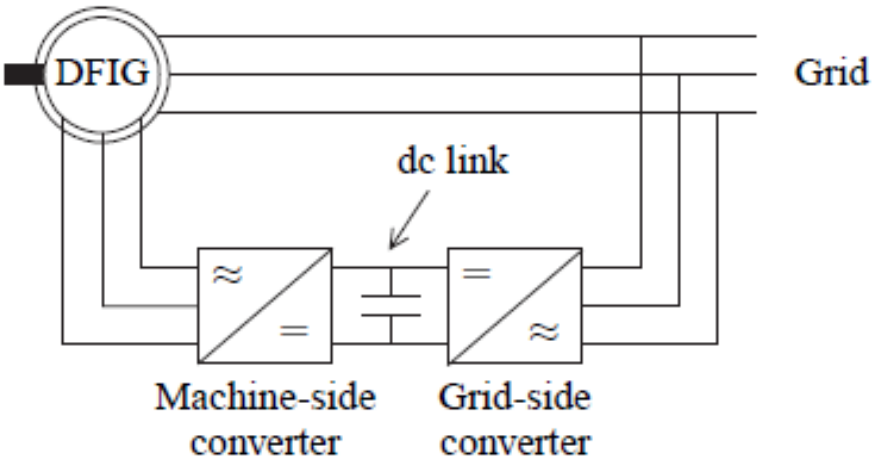

Figure 20: DFIG using a back-to-back converter[27, p.13]

Typically the DFIG system operates in a limited variable speed range at about ±30% for synchronous speed. Some other uses of the DFIG systems are flywheel energy storage system, stand-alone diesel systems, pump storage power plants, rotating converters feeding a railway grid from a constant frequency public grid [27, p.13-14].

5.2 Slip and angular frequency in DFIG

This chapter introduces the idea of which mode the DFIG can operate. The angular frequencies and slip of the generator determine which operational mode the DFIG uses. It can either be sub-synchronous, synchronous, or hypersynchronous mode (also called super-synchronous mod).

Angular frequency in the DFIG generator is given by [11, p.157]:

$$\omega_r = \omega_s - \omega_m \tag{15}$$

- ω_r is the angular frequency of the voltages and currents in the rotor windings(rad/s)
- ω_s is the angular frequency of the voltages and currents in the stator windings(rad/s)
- ω_m is the angular frequency of the rotor(rad/s)

ω_m is also given by[11, p.157]:

$$\omega_m = p * \Omega_m \tag{16}$$

Where Ω_m is the mechanical rotational speed at the rotor(rad/s)[11, p.157]

In regular steady-state operation, induced voltages and currents in rotor windings have ω_r angular frequency. The supplied external voltage in the rotor should also have ω_r angular frequency[11, p.157].

The relation between stator and rotor angular frequency speeds is commonly known as the slip[11, p.157]:

$$s = \frac{\omega_s - \omega_m}{\omega_s} \tag{17}$$

Combining equation 15 and 17, the relation between stator and rotor angular frequency and slip results in[11, p.157]:

$$\Omega_r = s * \omega_s \tag{18}$$

This also applies to the frequencies[11, p.157]:

$$f_r = s * f_s \tag{19}$$

Based upon the angular frequencies relations and slip, one can determine what mode the DFIG operates in[11, p.157]:

Operation Modes			
$\omega_m < \omega_s$	$\omega_r > 0$	$s > 0$	Subsynchronous operation
$\omega_m > \omega_s$	$\omega_r < 0$	$s < 0$	Hypersynchronous operation
$\omega_m = \omega_s$	$\omega_r = 0$	$s = 0$	Synchronous operation

Table 2: DFIG operation mode[11, p.157]

5.3 Equivalent circuit

Figure 21 shows the equivalent circuit of a doubly-fed induction generator, which also accounts for magnetizing losses. However, the Simulink simulations in Chapter 6-7 does not include magnetizing loss. The circuit is valid one equivalent Y phase and for steady state calculations. A δ-connected machine may also be represented by this Y circuit [27, p.14-15].

The DFIG circuit becomes the ordinary equivalent circuit for a cage-bar induction machine. By applying Kirchoff's voltage law to the circuit [27, p.14-15]:

$$V_s = R_s I_s + j\omega_1 L_{s\lambda} I_s + j\omega_1 L_m (I_s + I_r + I_{Rm}) \tag{20}$$

$$\frac{V_r}{s} = \frac{R_r}{s} I_r + j\omega_1 L_{r\lambda} I_s + j\omega_1 L_m (I_s + I_r + I_{Rm}) \tag{21}$$

$$0 = R_m I_m + j\omega_1 L_m (I_s + I_r + I_{Rm}) \tag{22}$$

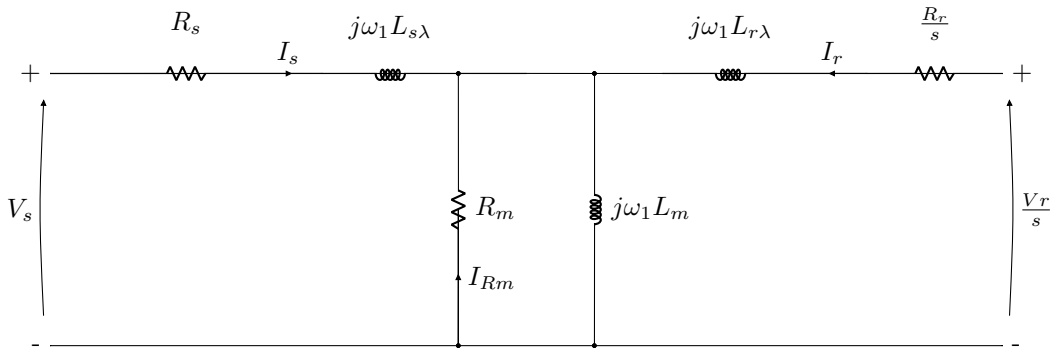

Figure 21: DFIG equivalent circuit[27, p.14]

Symbol	***Explanation***
V_s	Stator voltage
V_r	Rotor voltage
I_s	Stator current
I_r	Rotor current
I_{Rm}	Magnetizing resistance current
ω_1	Stator frequency
s	Slip
R_s	Stator resistance
R_r	Rotor resistance
R_m	Magnetizing resistance
$L_{s\lambda}$	Stator leakage inductance
$L_{r\lambda}$	Rotor leakage inductance
L_m	Magnetizing inductance

Table 3: Notations to Equivalent Circuit[27, p.15]

The slip (s) is calculated [27, p.14-15]:

$$s = \frac{\omega_1 + \omega_r}{\omega_1} = \frac{\omega_2}{\omega_1} \tag{23}$$

ω_r is the rotor speed, and ω_2 is the slip frequency. Air-gap flux, stator flux, and rotor flux are defined as [27, p.14-15]:

$$\psi_m = L_m(I_s + I_r + I_{Rm}) \tag{24}$$

$$\psi_s = L_{s\lambda}I_s + L_m(I_s + I_r + I_{Rm}) = L_{s\lambda}I_s + \psi_m \tag{25}$$

$$\psi_r = L_{r\lambda}I_r + L_m(I_s + I_r + I_{Rm}) = L_{r\lambda}I_s + \psi_m \tag{26}$$

Equivalent circuit equations [Eq. 20-22] can be rewritten [27, p.14-15]:

$$V_s = R_s I_s + j\omega_1 \psi_s \tag{27}$$

$$\frac{V_r}{s} = \frac{R_r}{s} I_s + j\omega_1 \psi_r \tag{28}$$

$$0 = R_m I_m + j\omega_1 \psi_m \tag{29}$$

Resistive losses can be calculated as follows [27, p.14-15]:

$$P_{Loss} = 3(R_s|I_s|^2 + R_r|I_r|^2 + R_m|I_{Rm}|^2) \tag{30}$$

Electro-mechanical torque [27, p.14-15]:

$$T_e = 3n_p I_m[\psi_m I_r^*] = 3n_p I_m[\psi_r I_r^*] \tag{31}$$

n_p is the number of pole pairs [27, p.14-15].

5.4 Some losses in DFIG

This section mentions some of the losses in the DFIG system. Implementing these losses have been essential to making the Simulink program more realistic. The simulation accounts for some of the most common losses.

5.4.1 Gearbox losses

Usually, the gearbox losses (in wind turbines) are caused by tooth contact and viscous oil losses. For simplicity, there are some assumptions made for simulations and calculations. The tooth losses are neglected, and viscous losses will be considered constant (Fixed percentage). A reasonable assumption is to calculate a viscous loss of 1% of rated power per stage. With this assumption, efficiency of the gearbox with "q" stages can be found with following equation [14, p.2] [15, p.574]:

$$Efficiency = \frac{P_{IntoGearbox} - q * 0.01 * P_{Rated}}{P_{IntoGearbox}} \tag{32}$$

5.4.2 Stray load losses

Chapter 4.5.4 defines the stray load losses in a generator. Additionally, IEEE 112 also defines it as: "The stray-load loss is that portion of the total loss in a machine not accounted for by the sum of the friction and windage loss, the stator I^2R loss, the rotor I^2R loss, and the core loss."[13, p.29]

An approximate equation of stray load loss can be written as:

$$W_s = 0.005 * \frac{P^2}{P_{Rated}} \tag{33}$$

In the equation, P is the generator output, and P_{Rated} is the rated power of the generator [31, p.3].

5.4.3 Stator losses

The size of the active stator power loss, Ps_{CuLoss}, is determined by the stator side per phase resistance R_S and the per phase current I_S [13, p.22-23] [11, p.166]:

$$Ps_{CuLoss} = 3 * R_S * |I_S|^2 \tag{34}$$

5.4.4 Rotor losses

The rotor side copper losses are calculated similarly to stator [11, p.166]:

$$Pr_{CuLoss} = 3 * R_R * |I_R|^2 \tag{35}$$

R_R is the rotor side per phase resistance and I_R is the per phase current.

5.4.5 Converter losses

The calculation method for converter losses in a DFIG system is similar to the one of PMSG in Chapter 4.5.5:

$$P_{ConverterLoss} = 0.03 * Pr \tag{36}$$

5.5 Brushless doubly fed induction generator

This configuration relies on the same principle as to modern slip-ring DFIG. The concept of dates back to the beginning of the 20^{th} century. The BDFIG has a provision of recovering slip power, without the need of slip-rings or carbon brushes. Dust generated from carbon brushes can in some applications become a long term problem. In a marine environment, the maintenance cost of DFIG is high due to slip rings and carbon brushes. Also, maintenance in marine areas is tedious and weather dependent[23, p.13].

The BDFIG is consists of two machines: main-and auxiliary/control machine. The main machine is grid-connected, while the two machine rotors connect in a cascade. Through a converter, the stator of the control-machine coupled to the grid. The slip power, of the main machine, is delivered to the grid through the control machine and the power converters. It increases efficiency due to slip power recovery. Also, it affects maintenance since slip-rings, and carbon brushes are not required. The converter size is also smaller compared to fully rated wind turbine converter systems. Also, this reduces harmonics injected to the grid and improves power quality[23, p.13].

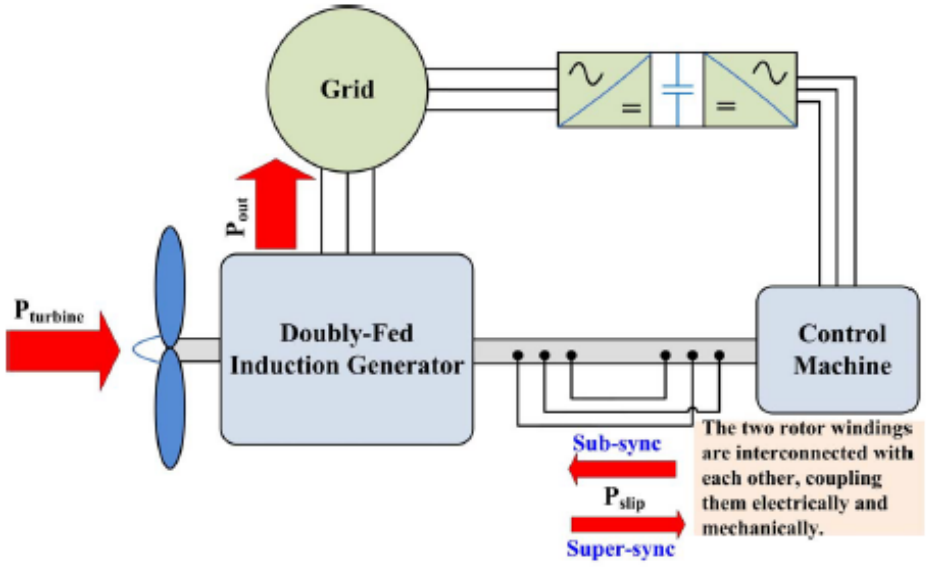

Figure 22: Brushless doubly fed induction machine[23, p.14]

There are two ways that main and control machines are connected:

- **The main and control machines connect in a non-inverted configuration**

  Most used in the early 20^{th} century. It allows for the machine to operate at three different speeds: around the synchronous speed of the main machine, around the synchronous speed of control machine and synchronous speed of the two machines connected in cascade. With this configuration, the stator of the main machine is connected to the grid directly, while the rotor connection through slip rings to the stator of the control machine. The control machine rotor is short-circuited, via slip rings [23, p.13-14].The main machine supplies its magnetization as well as that of the control machine [23, p.14].

- **The main machine connected in a non-inverted configuration, while the control machine is connected in an inverted configuration**

  The rotor of the main machine connects to the rotor of the control machine, which is similar to modern-day BDFIG. The use of variable resistor banks allows for variable speed control. However, since the control machine connect in an inverted configuration, two of the three rotor winding terminals are swapped and connected in reverse[23, p.14-15].

Integrating these two machines into one frame is called single-frame brushless doubly-fed induction machine (SF-BDFIM). Two ways of doing this are possible:

- The stator windings are mounted in one frame. It divides the stator into other segments. The primary and secondary windings are placed alternately in the stator, where the primary winding connects to the main. The secondary winding connects either to resistors or a converter for speed control. Since the stator windings have suitable spacing, their fields are not interlinked magnetically. They only connect through the agency of the rotor. This increases the machine size [23, p.15].

- The windings of the stator have the same iron path and are mounted in one frame. Both of the stator windings are inserted in the same slot. However, the number of poles must be different regarding the two stator windings to avoid direct coupling between them (transformer effect). In order to produce torque, the fields of the stator windings must only be coupled together through the rotor [23, p.15].

5.5.1 Modes of operating BDFIM

- **Cascade Induction Mode:** The machine has similar behavior to a typical induction machine, where speed changes with load. Both of the stators are linked magnetically via the rotor. One stator is grid-connected, while the other is stator is short circuited[23, p.15-16].

- **Cascade Synchronous Mode:** The main machine (Stator 1) connects to the grid, and the control machine (Stator 2) connects to the grid via electronic converters. Both of the stators need to be magnetically connected. A unique designed rotor ensures this. The purpose of the specially designed rotor [23, p.15-16]:

  The rotor induces currents (which produces a magnetic field), due to the currents in stator 1 (with p1 number of poles). The magnetic field in the rotor should have a harmonic component corresponding to the p2 number of poles. The p2 harmonic component couples with the p2 pole field in the winding of stator 2(having a p2 number of poles) [23, p.15-16].

  The currents in stator 2 will also induce currents in the rotor resulting in a magnetic field being produced by the rotor which contains a harmonic component of a p1 number of poles. The magnetic coupling between the rotor with stator 1, is now ensured. Therefore the machine can generate torque [23, p.15-16].

The power electronic converter system can control the varying torque, which is produced at constant speed [23, p.15-16].

Since the currents of the same frequency flow through both rotors, in the synchronous cascade operation, the following relation must be satisfied [23, p.15-16]:

$$\omega_m = \frac{\omega_1 + \omega_2}{p_1 + p_2}$$

ω_1 is the grid frequency and ω_2 is the frequency of the currents, being injected by the power electronic converter, connected to the stator of control machine [23, p.15-16].

5.5.2 Some drawbacks of the BDFIM

- High cost [23, p.15]
- Large size [23, p.15]
- Large weight [23, p.15]
- Low efficiency (Higher copper losses) [23, p.15]
- Low power factor, and lesser overload capacity [23, p.15]
- Increased magnetic leakage [23, p.15]

6 Grid faults and perturbations

This chapter addresses the challenges regarding perturbations on the grid and how it affects the wind generator system. The reason for including grid related faults is to see how it affects the operational conditions of the wind energy system. The DFIG Simulink program became a testing ground for studying this, but the issue of voltage dips and LVRT ability is addressed to PMSG aswell. Subsection 6.2 and 6.3 focuses on the DFIG model. The evaluation of LVRT is re-visited in Chapter 8, for both DFIG and PMSG.

6.1 Voltage dips and low voltage ride through

The earliest wind energy systems (such as the squirrel cage asynchronous generators) were poorly designed to withstand grid outages. If small disturbances occurred, the wind turbine would disconnect due to the tuning of the protection [11, p.46].

In order to avoid accidental disconnection to wind turbines, new control strategies must ensure the turbine:

- not to consume active power but remain connected to the power system during the fault [11, p.46]
- to assist recovery of voltage by providing reactive power during the fault [11, p.46]
- to assume normal operating conditions when the fault is over [11, p.46]

The definition to the demands mentioned above is *Low Voltage Ride Through(LVRT)*; Being able to ride through a fault (in the range of hundreds of milliseconds) consisting of a significant voltage drop[11, p.46].

The short-duration overcurrents (flowing through the power system) are the most common source of voltage dips. Any contributors to such currents are power system faults, motor startup, and transformer energizing. Also, single-phase short circuit is more typical for power system faults[11, p.48].

The voltage dips can be categorized into two groups:

- "Three-phase dips, when the voltages of the three phases fall into the same proportion"[11, p.50]
- Voltage is unbalanced, and the three-phase drops are unequal (Asymmetric dips):
  "Single-phase dips that affect only one phase"[11, p.50]
  "Biphasic dips that involve two phases"[11, p.50]

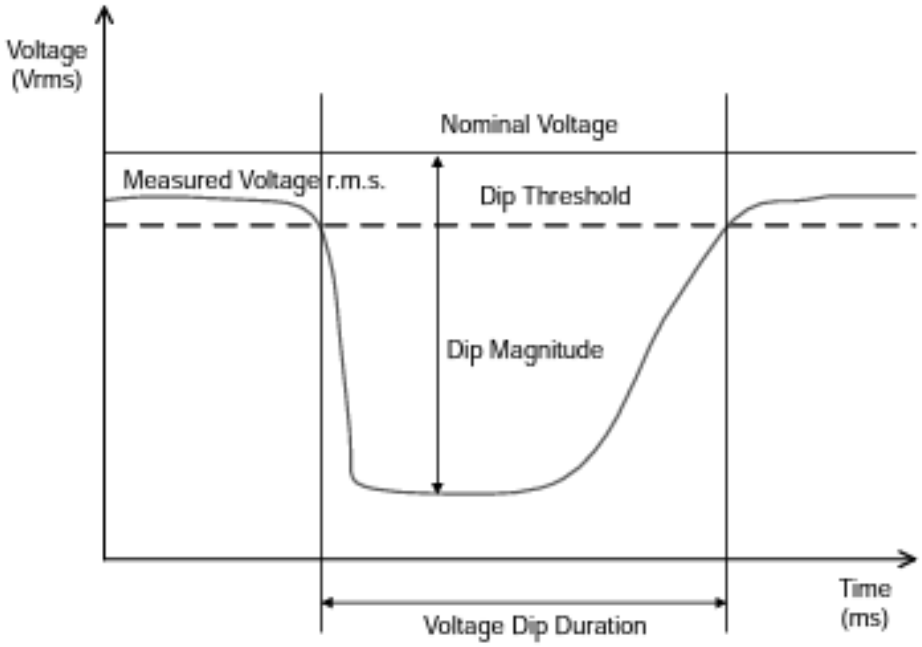

Figure 23: Voltage dip [11, p.51]

In Figure 23, the voltage dip is measured in RMS value and are calculated for each half-period($RMS_{1/2}$). The length of time, where the voltage is below 90%(of nominal value), is defined as the duration of the dip[11, p.50-51].

6.2 Crowbar

The crowbar is a protection device for power electronic circuits. It prevents overvoltages in their power supply by creating a low resistance path between the terminals (rotor terminals for DFIG) [11, p.481-484].

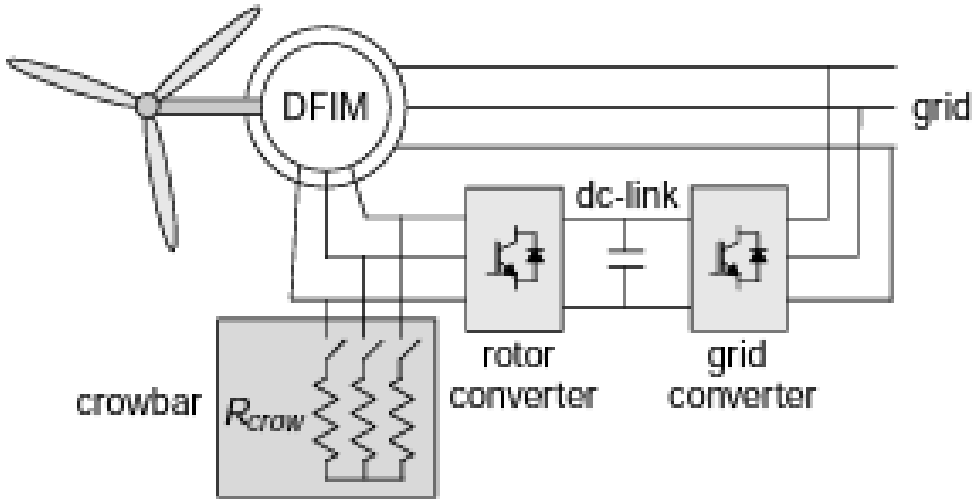

Figure 24: Simple crowbar [11, p.482]

The crowbar is activated if deviations like overcurrents in the rotor, overvoltages in DC-link or low stator voltages are present. In Figure 24, the currents from the rotor will be sent to the crowbar, and the rotor converter is switched off. The activation of the crowbar makes the circuit in Figure 25, work as an impedance divider. The converter voltage becomes a fraction of the EMF induced in the windings of the rotor. The configuration shown in Figure 24 consists of three resistances and bidirectional switches [11, p.481-484].

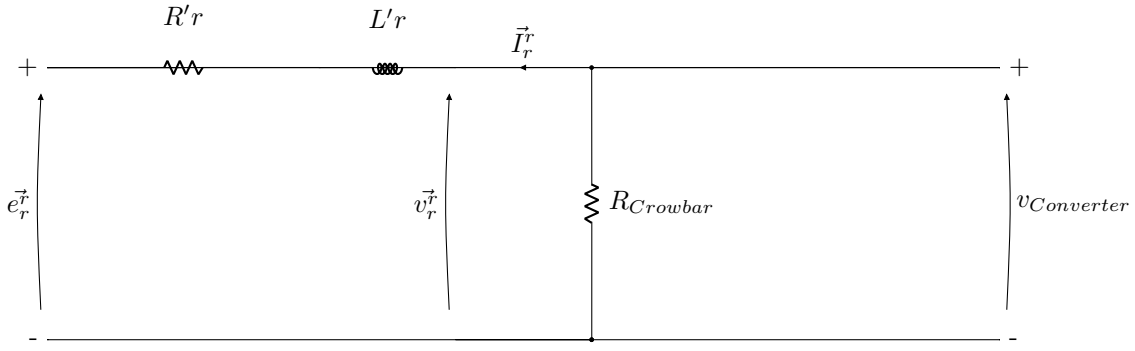

Figure 25: Equivalent circuit of simple crowbar configuration [11, p.482]

Other configurations of the crowbars also exist. Some variations used thyristors (SCRs) as switches. However, some problems occurred with them, such as not being able to control the cut-off (the thyristor remained connected until the circuit-breaker of the generator was activated). It resulted in disconnecting the generator from the grid[11, p.481-484].

Solutions resulting in generator disconnection from the grid is unwanted. New wind energy systems must be able to ride through the fault (Eliminating the short-circuit without generator grid-

disconnection). The active crowbar solves this issue by controlling both activation and deactivation. They include at least one switch with cut-off capability (GTO or IGBT's for example). With GTO or IGBT, it is possible to disconnect the crowbar and instantly reactivate the rotor converter so that the generator can resume normal operation [11, p.481-484].

6.3 Symmetric voltage dip simulation

The simulation is meant to show the effects of voltage dips on the DFIG system, how it influences the operational condition, and how the crowbar protection affects the voltage dip scenario (how it assists in achieving LVRT). However, the simulation has some assumptions:

- The voltage dip is symmetric
- The simulation neglects a realistic start-up (soft start) procedure of the wind turbine system(system starts at 0m/s and instantly increases to 8.5m/s)
- The DFIG losses are neglected (Ideal DFIG system)
- The voltage dip is programmed to activate in second 3
- The crowbar protection is programmed to quench the overcurrents instantly
- Simulation neglects the blade angle and direction of wind speed
- This model neglects transformer losses

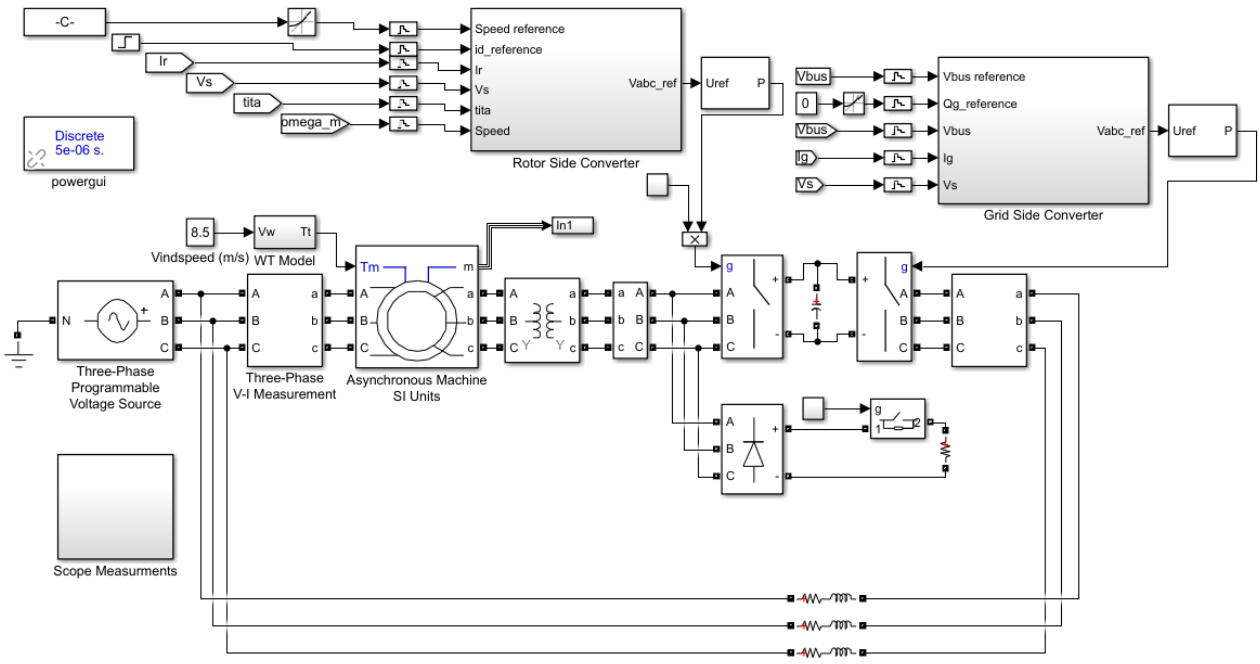

Figure 26: Simulink model with crowbar protection

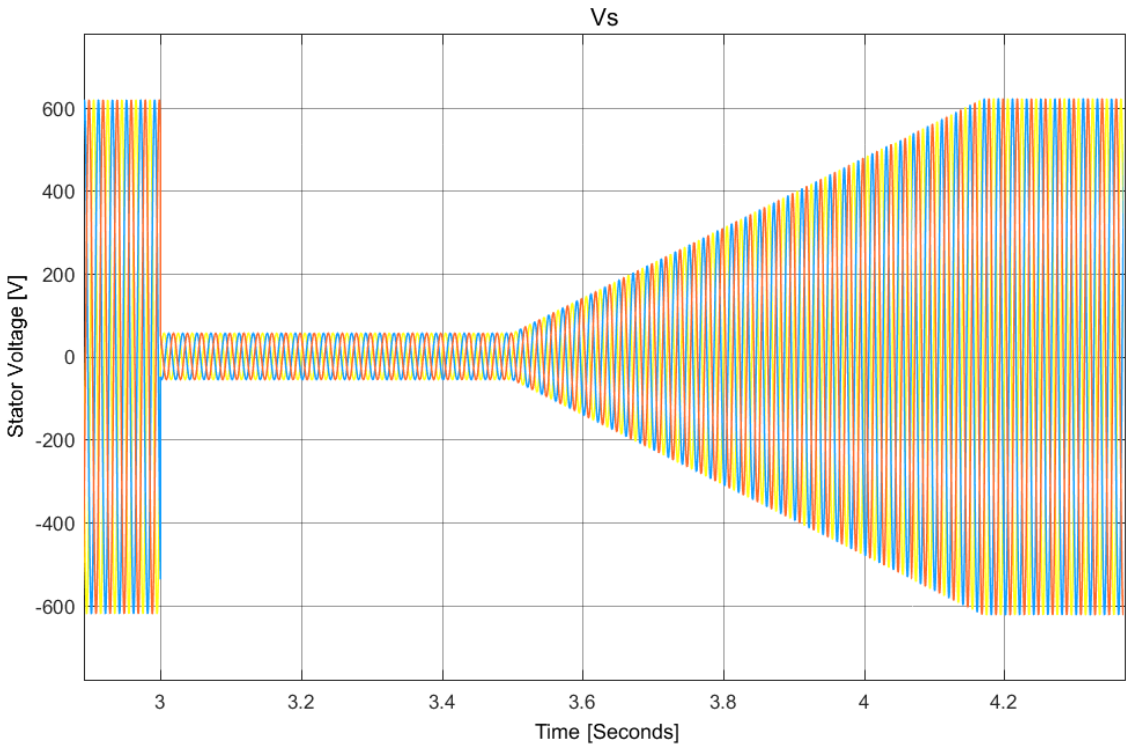

Figure 27: Stator voltage during the dip

Figure 27 show the voltage instantly decrease (from standard value to 10% of the nominal value) when the dip is triggered. The stator voltage remains at this value until it starts to recover proportionally with the stator flux (see Figure 29).

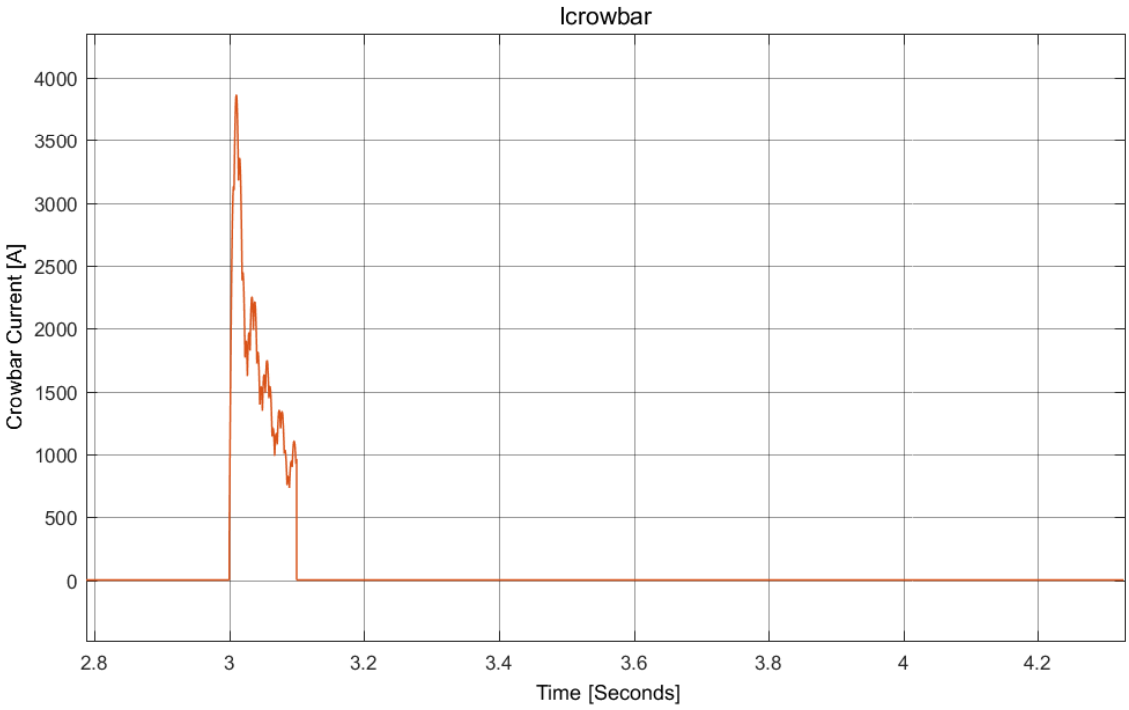

Figure 28: Crowbar current during the dip

As a result of the sudden stator voltage reduction, the rotor currents will drastically increase. The crowbar will sense these overcurrents, and lead them to an energy burn-off in the crowbar resistance. Figure 28 show the how the current quench occurs.

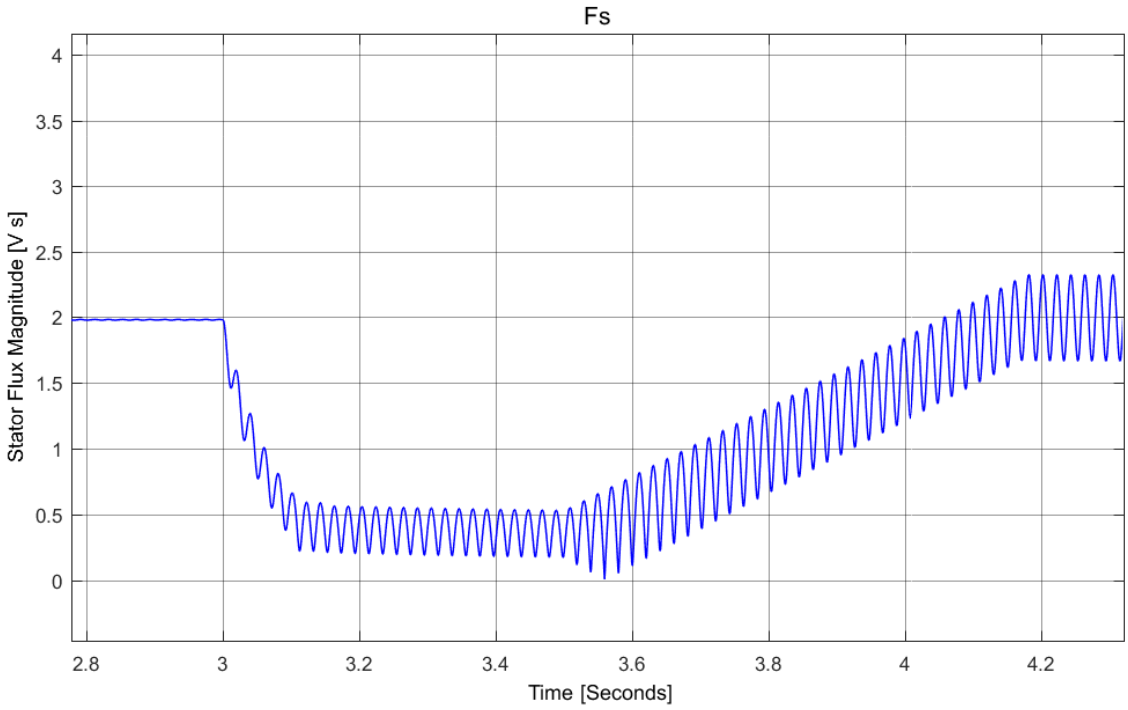

Figure 29: The stator flux amplitude

Figure 29 shows how the stator flux decays after the voltage dip is triggered. When the energy burn-off in the crowbar resistance has occurred, the stator flux returns to the nominal value.

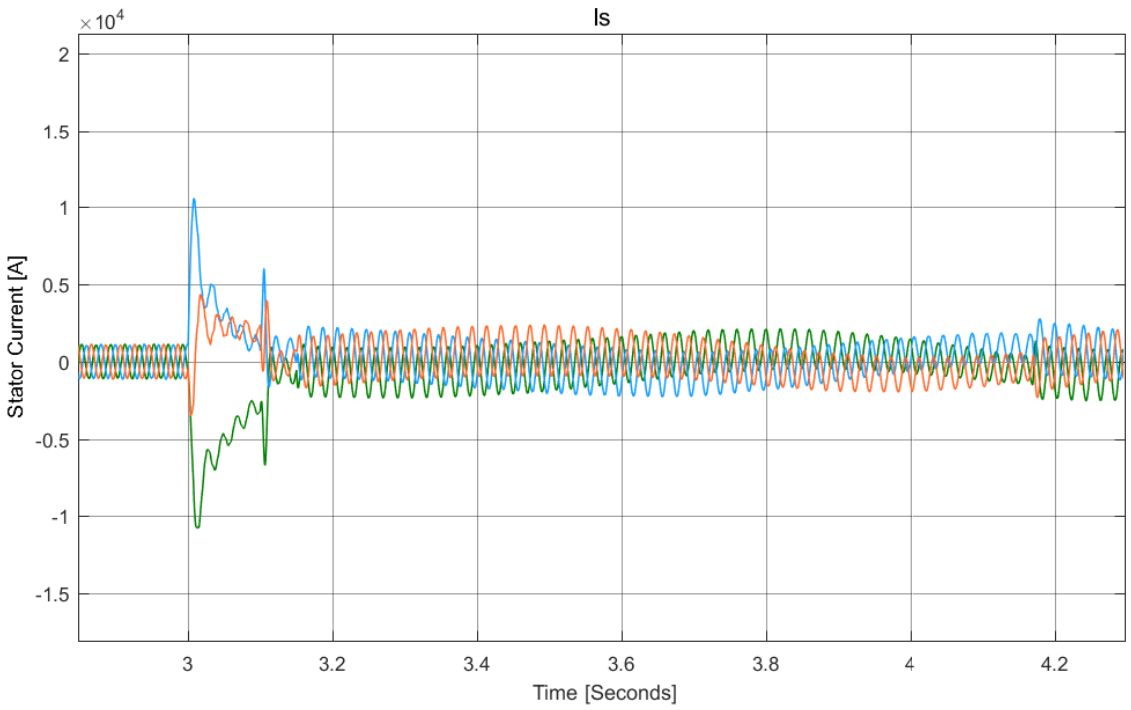

Figure 30: Stator current during the dip

When the voltage dip occurs, any control over the stator currents is lost. After the crowbar resistance has quenched the energy build-up, the stator currents will start to normalize again.

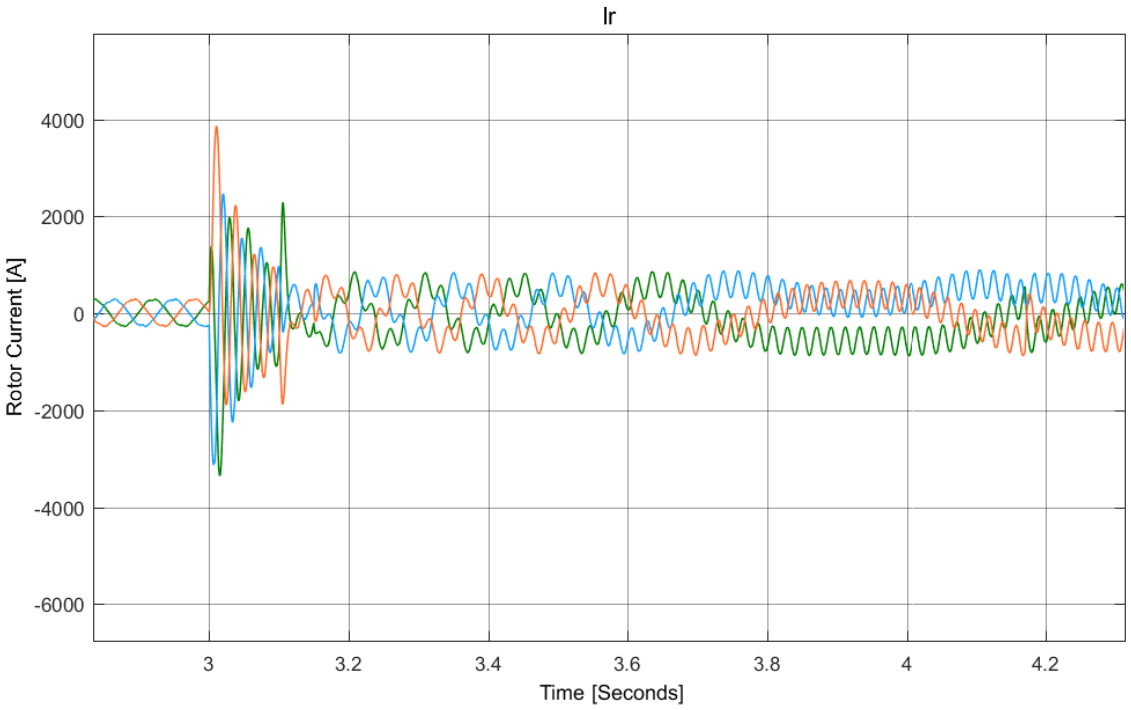

Figure 31: The rotor current during the dip

In Figure 31, it can be seen how the rotor current increases when the voltage dip is activated. The diversion of the overcurrent to the crowbar resistance makes sure the rotor side converter is now protected.

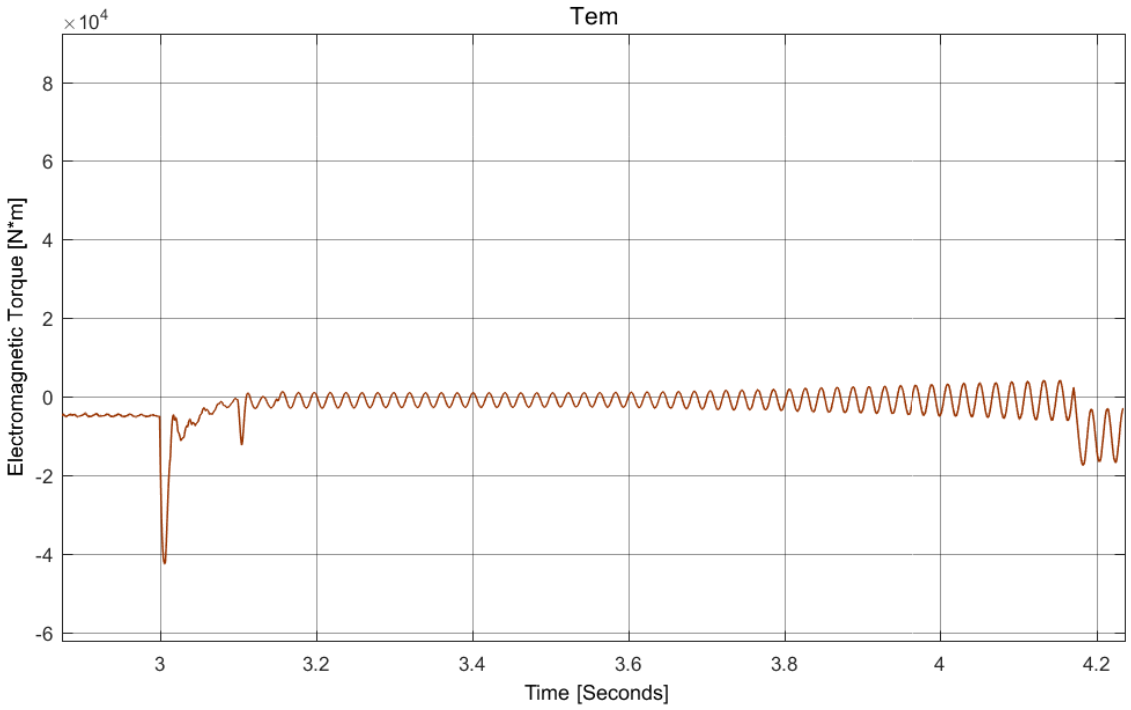

Figure 32: Electromagnetic torque

Figure 32 shows how the torque is at steady state and suddenly drops in response to the voltage dip. Some transients occur during the time of dip, but recovers and eventually stabilizes again.

7 DFIG Matlab testing

7.1 Introduction

The Simulink model is developed similarly to how Gonzalo Abad has demonstrated in his online lectures (and his book about Doubly Fed Induction Machines). His work has been essential for understanding and developing the simulations in this thesis(Chapter 6 and 7). Some information about his background is required:

"Gonzalo Abad received the B.Sc. degree in electronics from Mondragon University, Mondragon, Spain, in 2000, the M.Sc. degree in electrical engineering from the University of Manchester Institute of Science and Technology, Manchester, U.K., in 2001, and the Ph.D. degree from Mondragon University, in 2008.,Since 2001, he has been a Lecturer with Mondragon University. He has authored several papers and books in his research areas. He has participated in different industrial projects related to his research fields, and he holds several patents. His current research interests include renewable energies, power conversion, and motor drives." [16, p.1610]

7.2 DFIG parameters

The book "Doubly Fed Induction Machine: Modeling And Control For Wind Energy Generation" [11] had the necessary DFIG system parameters in order to develop a Simulink model. However, attempts to get these values from relevant manufacturer companies proved to be challenging due to restrictions and copyright.

Characteristic	***Value***	***Features***
Synchronism	1500rev/min	Synchronous speed at 50Hz
Rated Power	2MW	Normal stator three-phase active power
Rated Stator Voltage	690 V_{rms}	Line-to-line nominal stator voltage in rms
Rated Stator Current	1760 A_{rms}	Each phase nominalsttor current in rms
Rated Torque	12.7 kNm	Nominal torque at generator or motor modes
Stator Connection	Star	
p	2	Pair of poles
Rated Rotor Voltage	2070 V_{rms}	Line-to-line nominal voltage in rms
Rotor Connection	Star	
u	0.34	Stator/rotor turns ratio
R_s	2.6 $m\Omega$	Stator resistance
$L_{\sigma s}$	87 μH	Stator leakage inductance
L_m	2.5 mH	Magnetizing Inductance
R'_r	26.1 $m\Omega$	Rotor resistance
$L'_{\sigma r}$	783 μH	Rotor leakage inductance
R_r	2.9 $m\Omega$	Rotor resistance referred to the stator
$L_{\sigma r}$	87 μH	Rotor leakage inductance referred to the stator
L_s	2.587 mH	Stator inductance $L_s = L_m + L_{\sigma s}$
L_r	2.587 mH	Rotor inductance $L_r = L_m + L_{\sigma r}$

Table 4: Parameters for DFIG [11, p.179]

7.3 Simulink model

One of the crucial aspects of this thesis was to create a suitable model to run simulation tests. It has been challenging due to limited literature and manufacturer copyrights. Studies of relevant literature (books, articles, Ph.D.s) and online lectures have contributed to developing a DFIG simulation model.

The online guide mostly focuses on faults and behaviors of the DFIG. It includes simulations based on ideal conditions(no losses). However, it ignores power calculations, stator/rotor power calculations, efficiencies, and CP calculations. By adding these features, the Simulink model could emulate a more realistic wind energy system.

This simulation has the following assumptions:

- The losses included in the simulation is a result of the power block calculations. However, they are not physically placed in the simulation but systematically calculated from the wind turbine and towards the grid.
- This model neglects both transformer and cable losses.
- The simulation neglects a realistic start-up (soft start) procedure of the wind turbine system(system starts at 0m/s and instantly increases to pre-defined value)
- It is assumed a cut-in wind speed between 4.5-5m/s
- The rated wind speed is assumed to be at 12m/s
- The cut-off wind speed is assumed to be at 25m/s
- Simulation neglects blade angle and direction of wind speed
- The WT has a rated power of 2.6MW

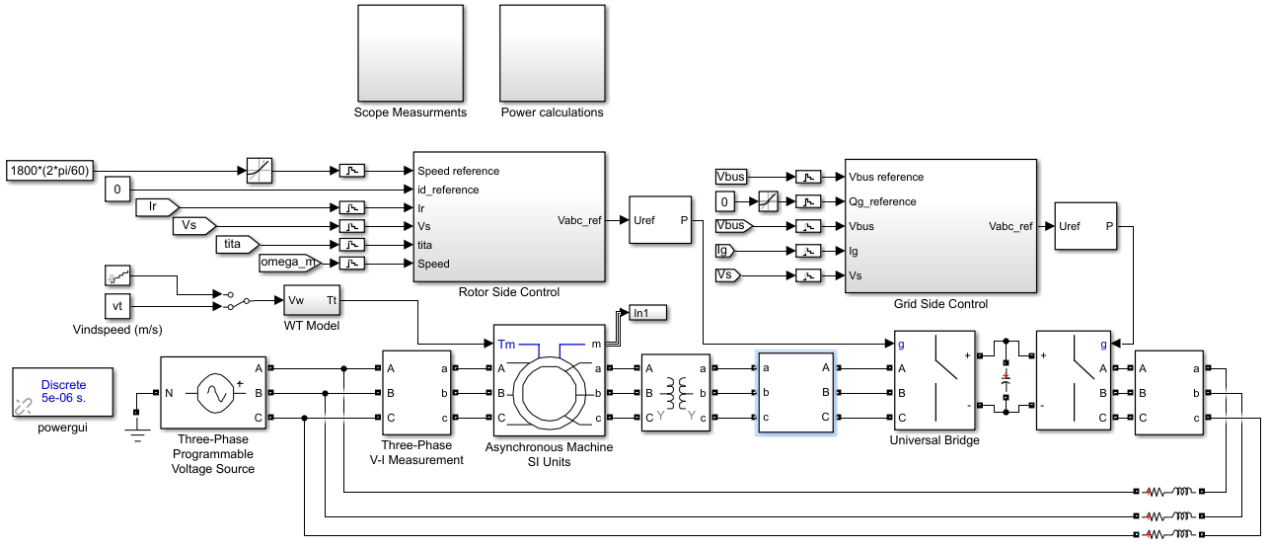

Figure 33: Simulink model

7.4 Explenation to figure 33

- In Figure 33, the WT-Model receives wind(m/s) as input and transforms this to torque. It is a simple WT-model but is sufficient for this simulation purpose.
- The Three-Phase Programmable Voltage Source emulates the overall power grid. The grid voltage is 690V with a frequency of 50Hz.
- The Asynchronous Machine(DFIG) receives torque from WT in order to produce power. The stator terminals are marked as A, B and C respectively, and are directly grid connected. Similarly, the rotor terminal markings are a,b, and c. The rotor circuit connects to the grid through the power converters.
- The grid side converter and the rotor side converter uses bidirectional switches, which converts voltage and currents from AC-DC-AC. Exchange of power is possible in both directions (Rectifier/inverter mode) depending on which mode the generator operates.
- Between the grid and the grid side converter, there is a filter(grid side filter). It is composed of three inductances (high filter is possible by adding capacitors to each inductance). In this model, the filter consists of a resistive and inductive part.
- The scope measurement block has been added to the simulation mainly to observe the DFIG operating conditions. It indicates how torque, mechanical speed, stator -and rotor voltages/currents, and converter bus-voltage develops under different operational scenarios.
- The power calculation block in is used to calculate the stator power, rotor power, all losses, stator/rotor currents, efficiencies, C_P, and total power. From start to stop, the displays in this block show the calculations of these values. The inputs for the power block are mechanical speed and torque (fed directly from the generator to the power block). Figure 34 gives a better image of the power calculation block.

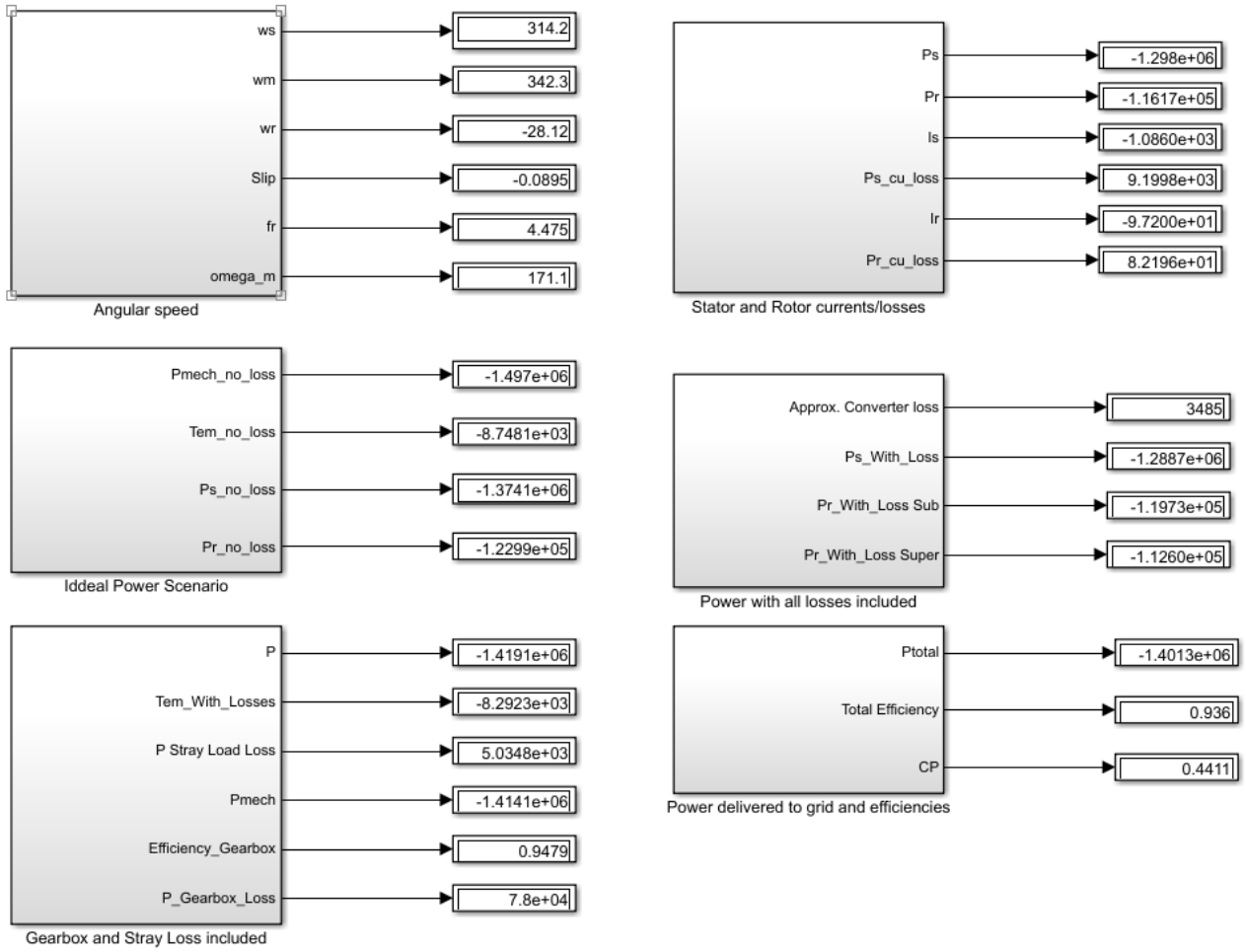

Figure 34: Simulink power block

7.5 DFIG simulation results

Simulink Results								
v (m/s)	4	5	6	7.5	8.5	9.174	10.5	12
ω_s (rad/s)	0	314.2	314.2	314.2	314.2	314.2	314.2	314.2
ω_m (rad/s)	0	210.9	211.7	257.3	291.2	314.2	359.2	410.2
ω_r (rad/s)	0	103.3	102.4	56.83	22.92	-0.03247	-45.01	-96.02
Slip	0	0.3288	0.3260	0.1809	0.07295	-0.0001	-0.1433	-0.3056
Ω_m (rad/s)	0	105.4	105.9	128.7	145.6	157.1	179.6	205.1
Pm_{NoLoss} (W)	0	-155000	-320600	-631100	-920700	-1156000	-1736000	-2589000
Tem_{NoLoss} (Nm)	0	1469.8	-3028.8	-4904.9	-6322.5	-7357.9	-9665.8	-12625
Ps_{NoLoss} (W)	0	-230870	-475760	-770460	-993140	-1155800	-1518300	-1983200
Pr_{NoLoss} (W)	0	75907	155120	139380	7244.5	-119,45	-217530	-606120
$P_{StrayLoss}$ (W)	0	14.808	147.19	764.75	1775.3	2904.6	6871	15766
$P_{GearboxLoss}$ (W)	0	78000	78000	78000	78000	78000	78000	78000
I_{Stator} (A)	0	-95.923	-301.07	-564.21	-759	899.39	-1208.3	-1599.3
I_{Rotor} (A)	0	31.538	98.159	102.07	55.365	-0.0929	-173.12	-488.8
Ps_{CuLoss} (W)	0	71.77	707	2483	4493.4	6309.5	11388	19950
Pr_{CuLoss} (W)	0	8.6536	83.826	90.632	26.668	-0.00007	260.74	2078.7
$P_{ConverterLoss}$ (W)	0	1131	3519	3659	1985	3.333	6207	17530
$Ps_{WithLoss}$ (W)	0	-114570	-359100	-671820	-902600	-1068600	-1432700	-1891400
$Pr_{WithLoss}$ (W)	0	36553	113710	118230	64156	-107.76	-200430	-564570
P_{Total} (W)	0	-78015	-245390	-553590	-838440	-1068700	-1633100	-2456000
Efficiency	0	0.5034	0.7653	0.8772	0.9107	0.9245	0.9408	0.9485
CP	0	0.3652	0.4373	0.4407	0.4417	0.441	0.4418	0.4414

Table 5: DFIG simulations at different wind speeds

Table 5 accounts for the most significant measurement values. The power calculations in the Simulink power block use the grid side voltage (690V) as a reference value. Appendix A describes the notations and the Simulink calculations used in table 5.

The DFIG system delivers maximum -2456000W to the grid, at the rated wind speed (12m/s). At this production level, the system is close to reaching its mechanical and electrical limit. The simulation uses a max power block, which locks the max power value if using higher input windspeeds. In reality, exceeding max wind speed may result in overheating and mechanical faults to occur.

The values presented in table 5 is the result of simulating at different wind speeds through many simulations. One simulation consisted of a wind speed of 5m/s, another at 6m/s, eventually reaching 12m/s. Additionally, a timer block was added, which changes the wind speed at a specific time. The results could be graphically presented, after plotting them int Excel. Efficiency/power values from wind speeds above 12m/s were not measured in the Simulink model but calculated in Excel and included in Figure 33-38.

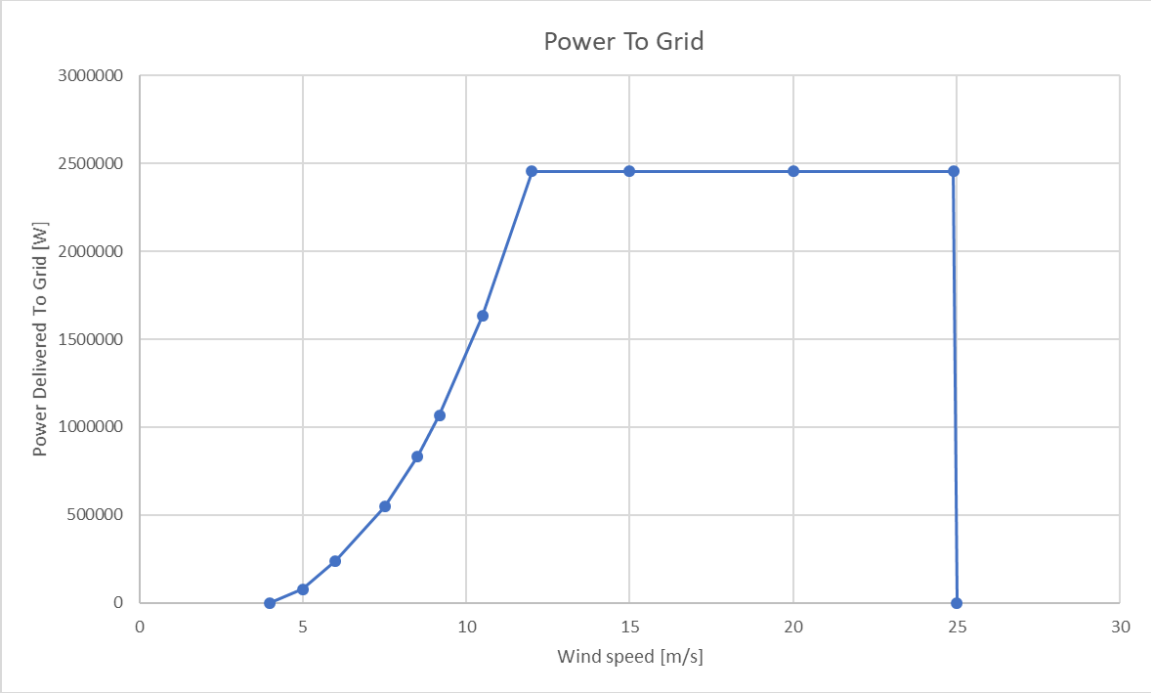

Figure 35: Total power delivered to the grid

Figure 35 shows the total power delivered to the grid. The cut-in speed of the system is 4.5-5m/s, the rated speed is 12m/s and the cut-off speed is at 25m/s. Figure 35 includes all losses.

Both Figure 35 and 36 operates in generator mode. However, they are presented with positive signs to give a better overview.

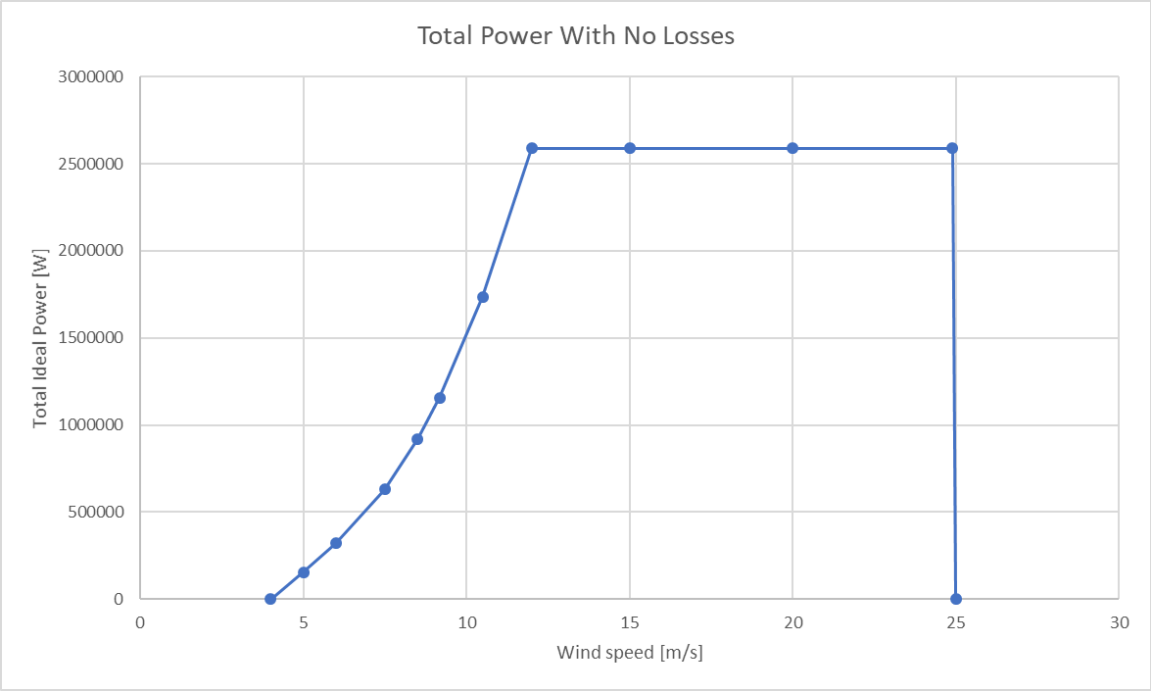

Figure 36: Power production with ideal assumptions

Figure 36 shows the power curve under ideal assumptions and does not include losses. However, it results in a higher total power up to almost 2.6MW. The assumption in Figure 36 is:

$$Pm_{NoLoss} = Ps_{NoLoss} + Pr_{NoLoss}$$

The reason for including Figure 36 is simply for comparing it to Figure 35, and visualize how losses affect the total power production.

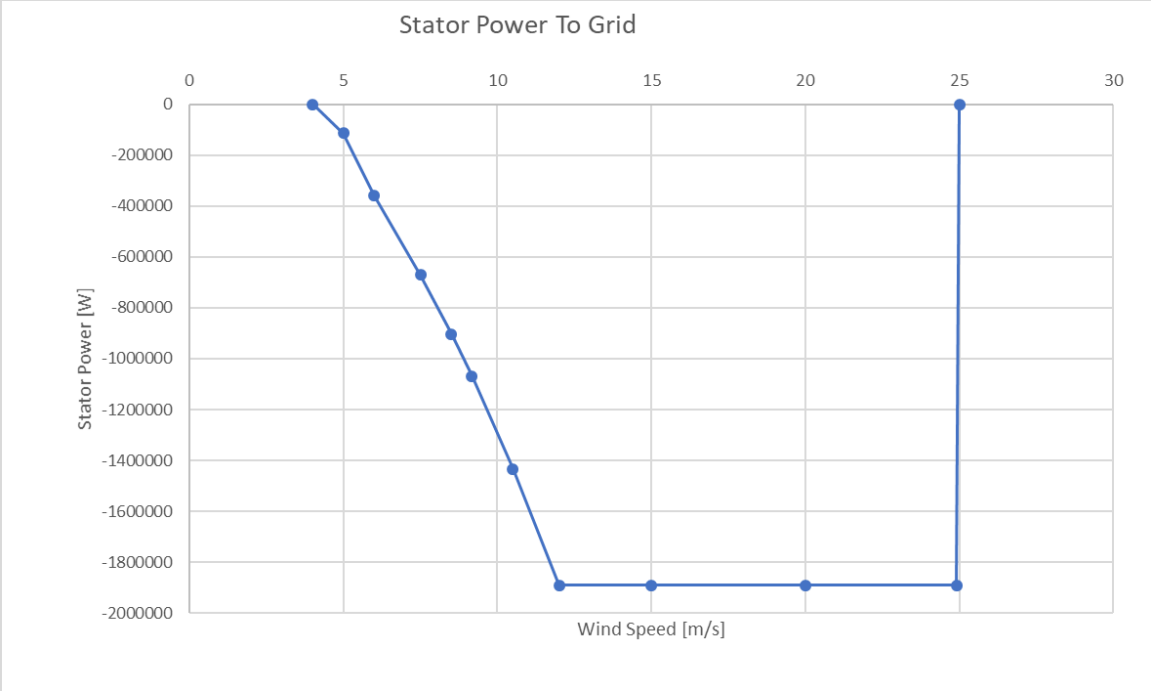

Figure 37: Stator power delivered to the grid

Figure 37 shows the stator power delivered to the grid, at different wind speeds. Since the stator delivers power to the network, the values have a negative sign.

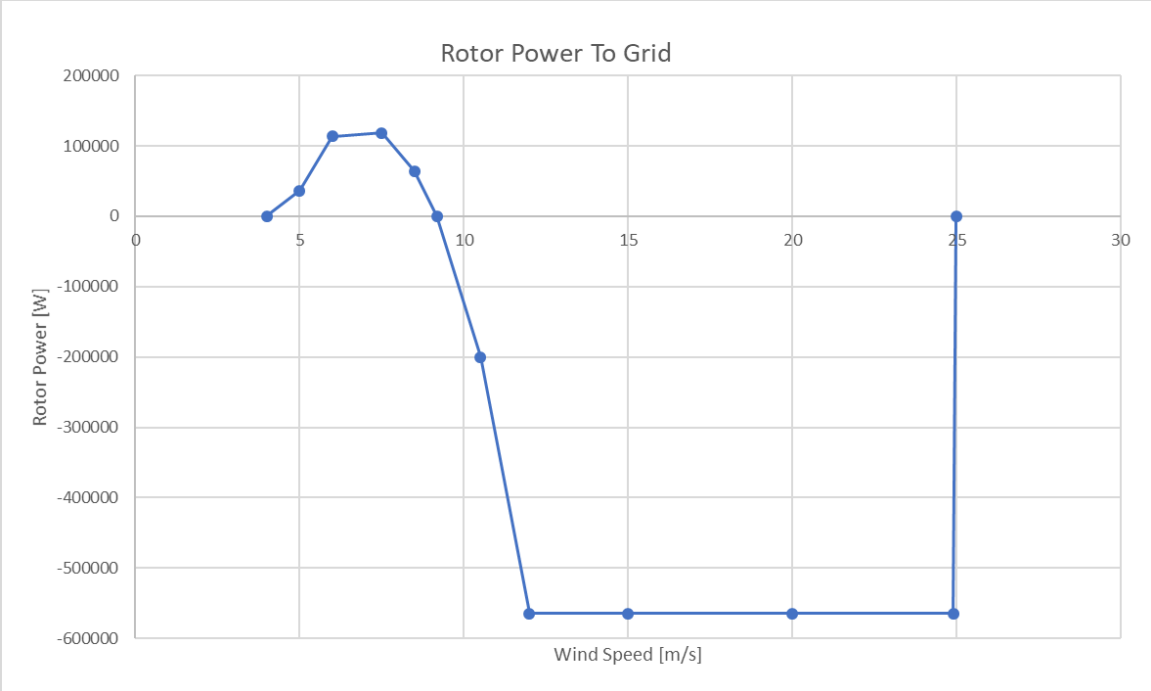

Figure 38: The rotor power development (from subsynchronous to hypersynchronous operation)

Figure 38 (rotor power development) reveals how generator modes change during different wind speed scenarios. The generator starts at subsynchronous mode, where the rotor consumes power (power signs are positive). At synchronism, the rotor either delivers or consume power (happens at a wind speed of 9,175m/s). Supersychronism(Hypersychronism) starts when the rotor delivers power to the grid.

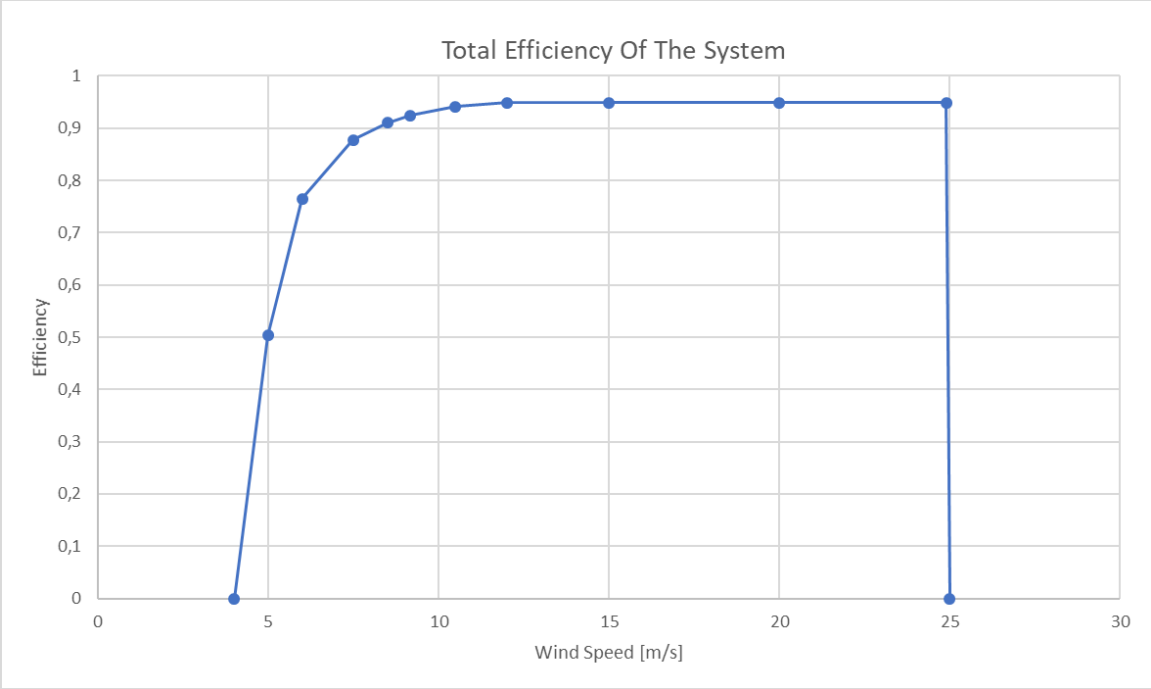

Figure 39: The total efficiency of the system

The efficiency in Figure 39 is found by dividing P_{Total} with Pm_{NoLoss}(Total power produced/Power produced at WT). The efficiency increases until reaching the rated wind speed (12m/s). At this point, the system has achieved max power production, and the total efficiency will remain relatively constant until cut-off speed.

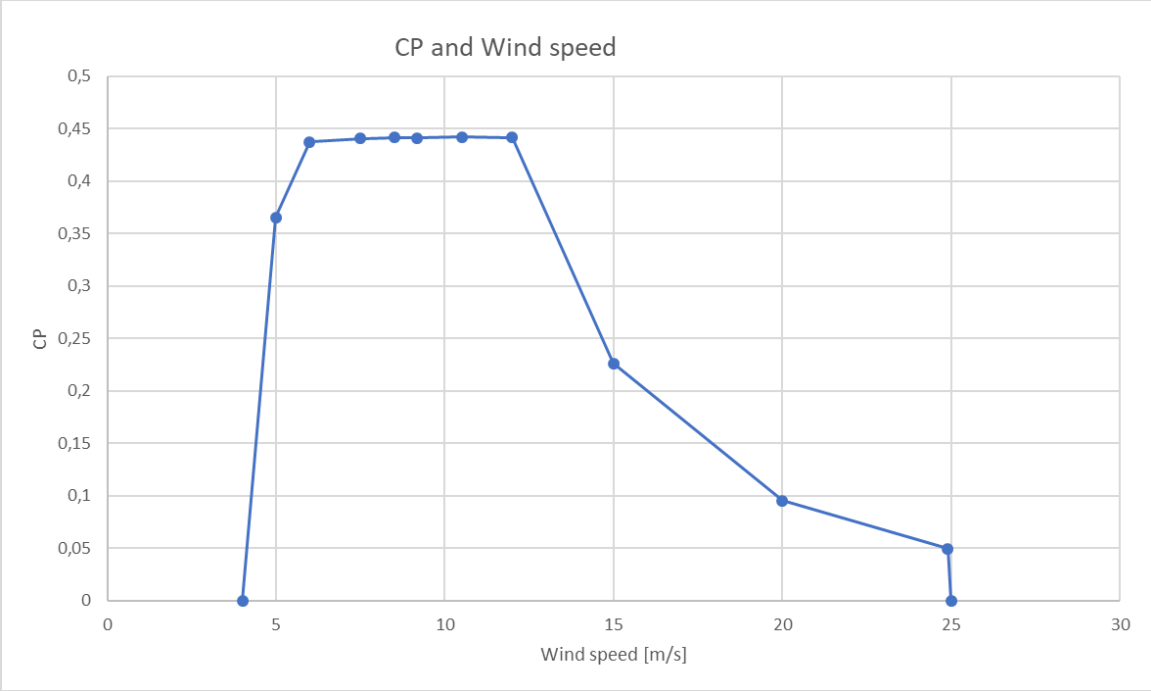

Figure 40: How C_P develops at different wind speeds

Figure 40 shows the development of C_P during different wind speed scenarios. At about 6-12m/s, the wind to power transformation is high. As the system reaches its max power production, the C_P will decrease with higher wind speeds. At 12-25m/s this becomes visible.

8 Comparison of generator configurations

8.1 Introduction

As mentioned in Chapter 1.2, this thesis focuses on the comparison between the DFIG and SG, more specifically, the PMSG.

Subchapter 8.2-8.4 discusses each system with regards to:

- Efficiency
- Operating condition
- Economic Perspective

However, economic evaluation has proven difficult since most manufacturers have restrictions on sharing any information regarding their products. In subchapter 8.5, a table is designed to summarize the different properties for each system. Subchapter 8.6-8.7 gives a conclusion for this thesis and some ideas for further work.

8.2 Efficiency

The efficiency of the generator system has always been a topic of discussion and debate regarding loss reduction and productivity optimization. When considering how to evaluate the efficiency of a wind energy configuration, the following components are essential:

- The efficiency of the gearbox
- The efficiency of the generator
- The efficiency of the converter

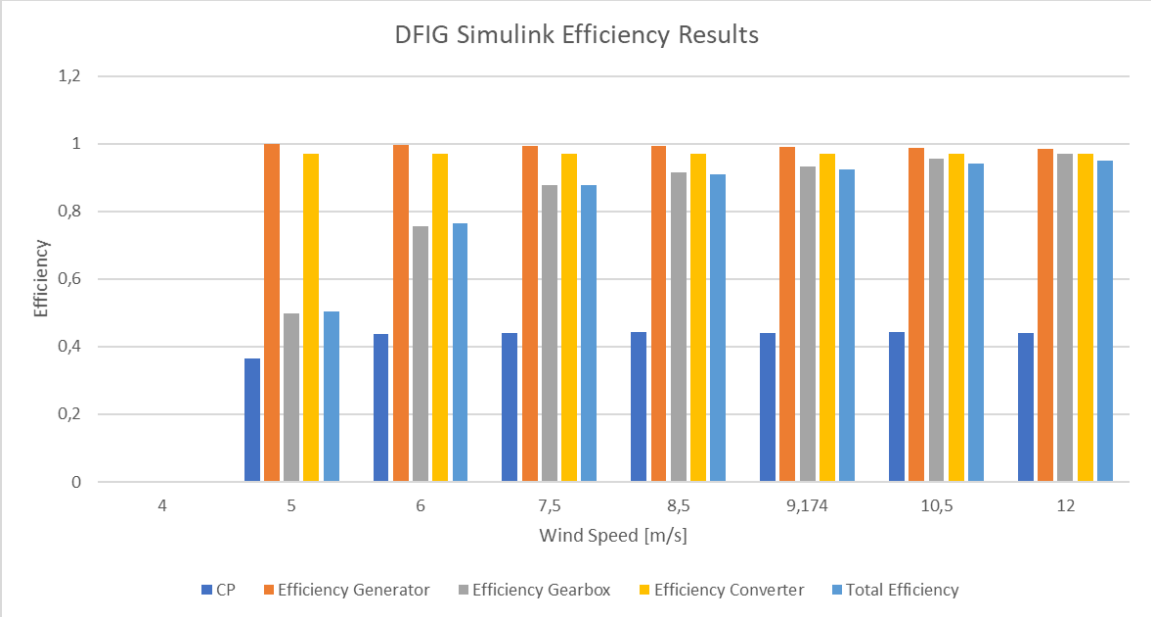

Figure 41: Representation of the DFIG efficiencies from Simulink

Figure 41 presents the efficiency results from the DFIG simulations in this thesis. It includes the gearbox, generator, converter, total efficiency, and the C_P factor.

8.2.1 DFIG

- **Gearbox**

A known issue with the DFIG configuration is the need for gearbox implementation. It represents an additional power loss, which also affects the total efficiency of the system (it also needs regular maintenance). The losses from gearbox usually increase with higher wind speeds. When exposing the system to high wind speed over time, the probability of gear and bearing faults also increase[19, p.3].

- **Generator**

The DFIG generator efficiency is typically affected by the stray load, iron, and copper (stator and rotor) losses. These are the most known losses and have been a subject of study, by several authors and researchers. Chapter 5 mentions some of these losses. The simulation resulted in several efficiency values at different wind speeds. From Figure 41, the average efficiency of the generator is at 97-99%. ABB's brochure states an efficiency of 97-97.5% [1].

However, the DFIG generator technology is the most dominant choice for new (onshore) wind energy systems today, and its high efficiency is one of these reasons.

- **Converter**

Converter rating for DFIG systems is about 25-30%, compared to 100% of the total nominal power of the generator. The converter losses for DFIG systems are smaller, compared to that of a fully rated converter generator system. Also, it helps the system achieve a smooth grid integration.

The efficiency of a DFIG converter is typically between 97-98% [2].

8.2.2 PMSG

- **Gearbox**

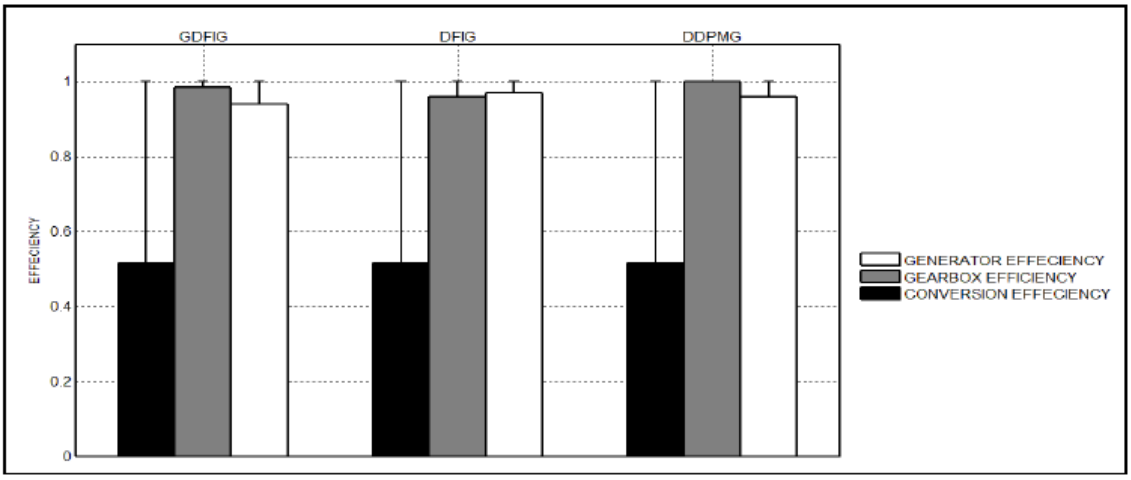

Figure 42: Efficiency analysis of several wind energy systems[28, p.308]

Direct driven PMSG configuration has no gearbox in its system. It is a significant advantage since losses from gearbox can be neglected entirely. Figure 42 shows an analysis which also debates the efficiency of wind energy systems. Gearbox efficiency with direct drive configuration can be set equal to one (100% efficiency). No gear maintenance is required.

Both the medium and high-speed wind generators use gearboxes. The losses will (in such case) be present, and the total efficiency is affected by it.

- **Generator**

PMSG generators have in general lower losses since there are no excitation losses [9, p.2]. Any information about the efficiency of the direct driven permanent magnet synchronous generators on ABB's webpage and brochures proved unsuccessful. However, they have high efficiencies, and another comparison article [28, p.308] suggest up to 96% efficiency [4][7].

ABB's brochures for medium and high-speed generators, reveals efficiencies at 98% [4, 7].

- **Converter**

The converters used in the PMSG system has (compared to DFIG) larger power rating. The converter must handle the same amount of power which the generator can produce at maximum power production. It also results in higher power losses. Components used in the converters must also be designed to handle higher power flows. Efficiency on the converters remains somewhat the same as for DFIG [1].

8.2.3 Sintef efficiency analysis of wind energy systems

The components included in the analysis from the Sintef article is [24, p.5]:

- Gearbox
- Generator
- Converter
- Transformer (This thesis does not include transformer losses)

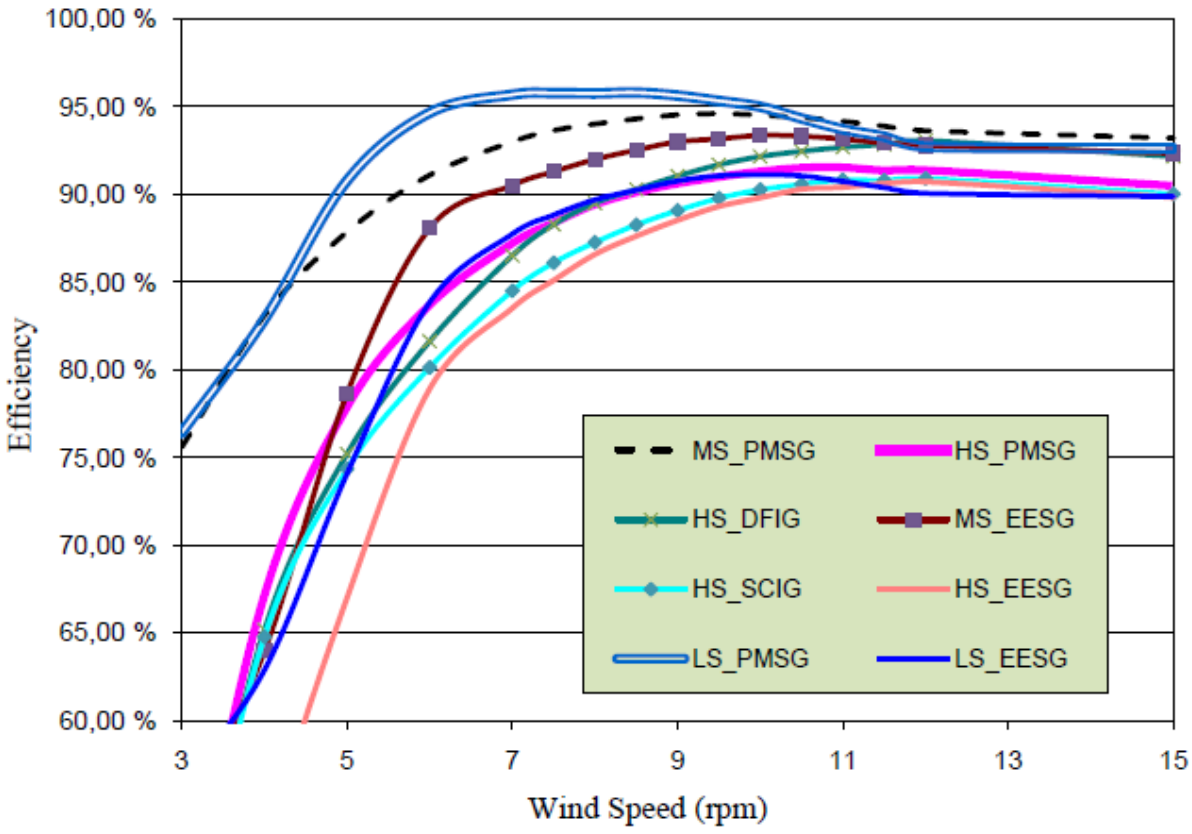

Figure 43: Sintef efficiency analysis of several wind energy systems [24, p.5]

Definitions to Figure 43:

- LS - Low Speed
- MS - Medium Speed
- HS - High Speed
- PMSG - Permanent Magnet Synchronous Generator
- DFIG - Doubly Fed Induction Generator
- EESG - Electically Excited Synchronous Generator
- SCIG - Squirel-Cage Induction Generator

As the figure from this analysis, the direct driven permanent magnet synchronous generator solution gives highest peak efficiency(followed by the MS PMSG) at wind speeds up to 15m/s [24, p.5].

8.3 Operating conditions

When installing wind generator systems, its ability to function normally under challenging and different conditions are crucial both for long term efficiency and cost-effectiveness. If not correctly designed (depending on environment and protection systems), instability or damage to certain parts is more likely to occur. The operating condition for a wind energy system is one of the essential evaluations since it determines how well a system should function during grid faults or voltage dips(as an example). If the designed system is unable to handle specific perturbations that may occur, unrepairable damage to the system is a possible scenario.

LVRT is essential regarding the evaluation of the operating condition of DFIG and PMSG systems. However, the following citation from Chapter 6 explains this:

"In order to avoid accidental disconnection to wind turbines, new control strategies must ensure the turbine:

- **not to consume active power but remain connected to the power system during the fault**
- **to assist recovery of voltage by providing reactive power during the fault**
- **to assume normal operating conditions when the fault is over"**

8.3.1 DFIG

The doubly-fed induction generator system is more exposed to grid faults since stator connects directly to the electrical grid. Only the rotor circuit is isolated through the power converters[26, p.3-4].

In the case of significant voltage dips at the wind turbine terminal, high transient currents in the stator and consequently the rotor (magnetically coupled) will occur. The energy build-up may result in damage to the rotor side converter and cause a sizeable DC-link voltage (in the power converter)[26, p.3-4].

It makes the DFIG configuration very dependent on protection systems, in order to handle such perturbations when they occur. The crowbar protection is one such fail-safe, which prevents the rotor current build-up from damaging the rotor side converter (see Chapter 6). Also, it is possible to install a DC-chopper (placed in the DC-link of the power converter, in parallel to the capacitor) as an additional safety precaution. It limits the energy build up in the DC-link (but do not influence the rotor current build-up) [34, p.423][26, p.3-4].

Figure 44 gives an overview of how the DFIG system could be protected from faults[26, p.3-4].

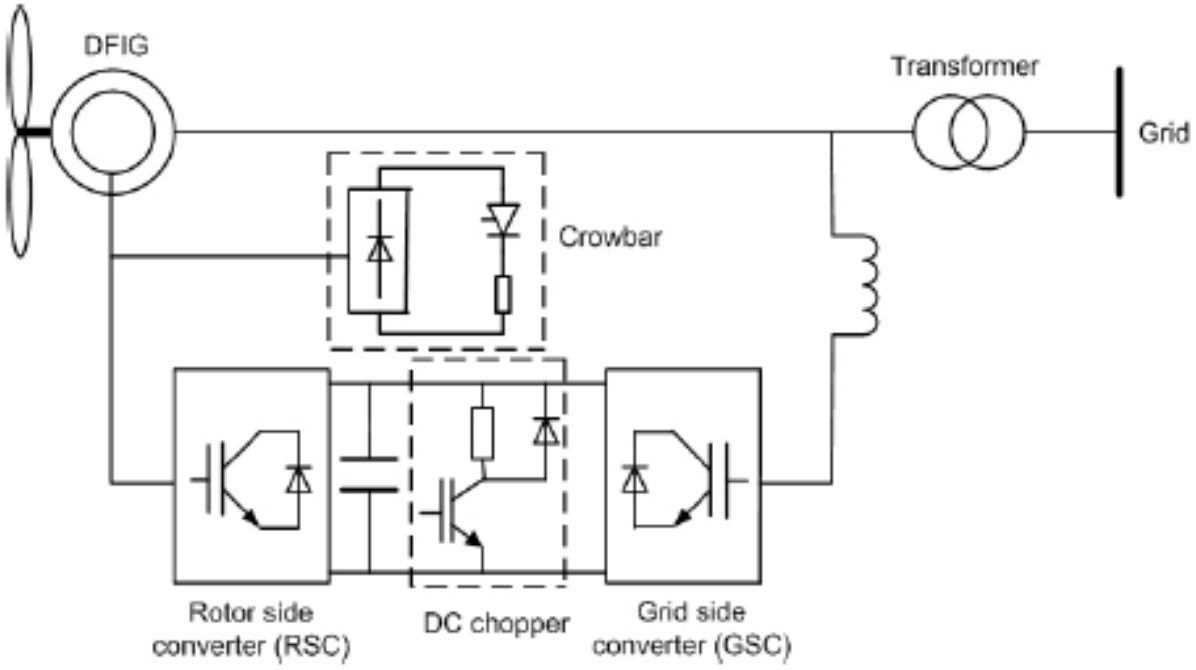

Figure 44: DFIG system with crowbar and DC-chopper[26, p.3-4]

A possible solution for preventing the grid fault is to modify the converter control (Often used in addition to crowbar protection). When applied to the rotor side converter and grid side converter, one can decrease peak values of the rotor currents and DC-link voltages, and deliver reactive power into the grid. Also, it contributes to re-establish the voltage during the fault[26, p.3-4].

8.3.2 PMSG

The PMSG system consists of fully rated power converters. It decouples the PMSG entirely from the grid, resulting in grid-related faults being "disconnected" from the generator-turbine system. Similarly to the DFIG, PMSG system can contribute to voltage re-establishment by injecting reactive power to the grid. However, the (PMSG) converters can supply more reactive power than the DFIG system during faults[26, p.4-5].

When grid perturbations occur, the terminal of the wind turbine experiences a voltage drop. The maximum amount of active power delivered to the grid will decrease in proportion to the reduction of voltage. With this outcome, the active power of the grid side converter supplied to the grid also drops by the converter controllers. If input power from the generator is unable to be reduced quickly enough, an energy imbalance in the converters occurs. Also, this results in a voltage build-up in the DC-link that may damage the converters [26, p.4-5].

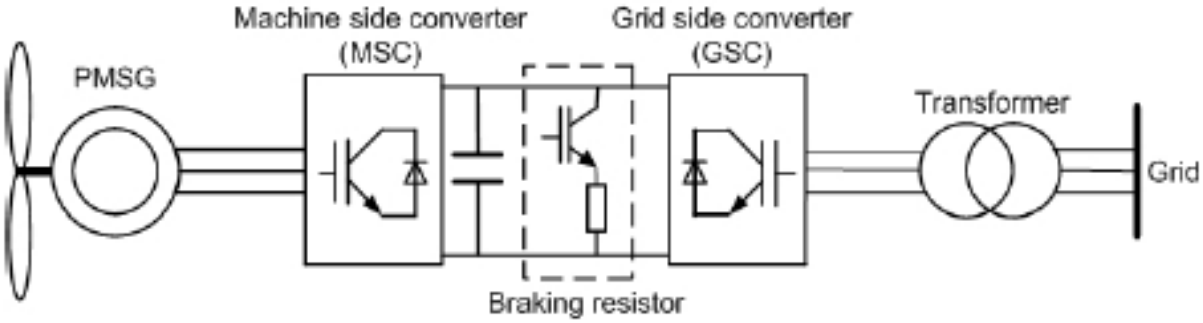

Figure 45: PMSG system with electromagnetic braking resistor [26, p.4-5]

In Figure 45 an electromagnetic braking resistor, controlled by a power electronics switch, have been used in order to dissipate the excess energy in DC-link. It prevents the DC-link overvoltage build-up during faults and protects the DC-link capacitor [34, p.423] [26, p.4-5].

8.4 Economic perspective

The economic perspective of wind generator systems (as mentioned in the introduction of this chapter) has proven challenging with regards to prices of each system. This thesis will not conclude any specific prices or numbers to this, but rather indicate if one system is initially more expansive or not through related research.

Total cost of three different generator systems			
Cost (KEuro)	SCIG	DFIG	PMSG
Gearbox	220	220	0
Converter	120	40	120
Generator Cost	287	320	432
Total Cost with margine for company costs	1837	1870	1982
Annual energy yield (MWh)	6705	7690	7890
Annual energy yield/Total cost	3.63	4.11	3.98

Table 6: The estimated cost of several wind energy systems [19, p.5]

Some articles give an economic evaluation of the DFIG and PMSG system, like table 6. As the table suggests, the initial cost of the PMSG is higher than the other two systems.

In most land-based (onshore) wind parks the DFIG system is still the favorite due to the lower cost of the converter since its size only rates 30% of total power.

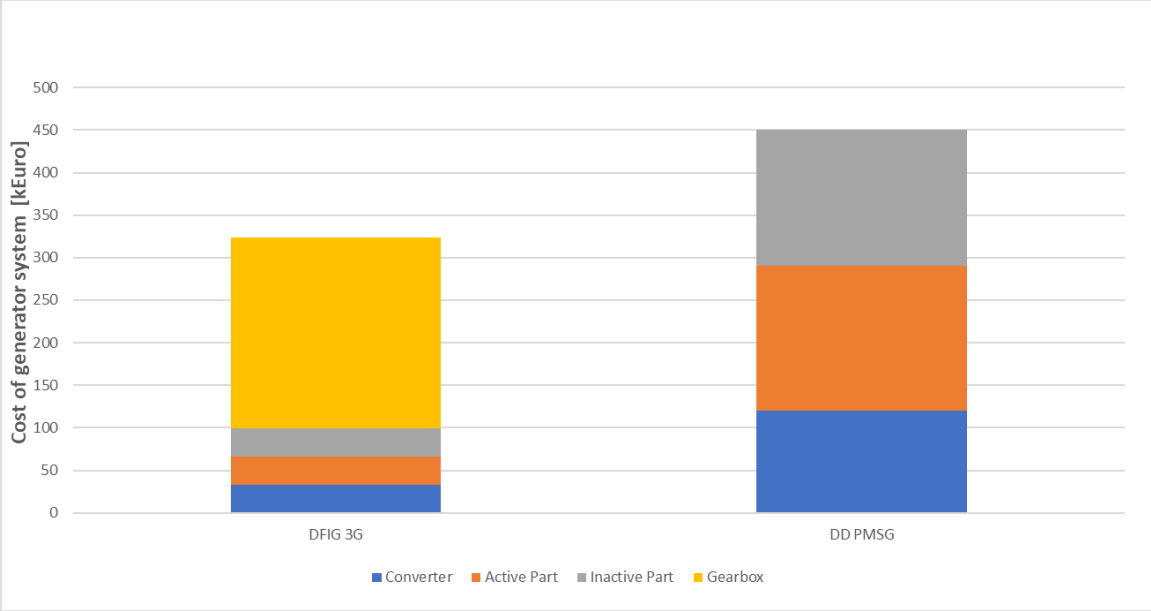

Figure 46: Cost of 3MW DFIG and PMSG generator systems [18, p.2]

Figure 46 cost estimation where the DD PMSG and DFIG with a 3-stage gearbox are presented. The economic evaluation divides each system into the gearbox, inactive part, active part, and converter [18, p.2].

However, maintenance costs also play an essential role in each system, where the DFIG system has some challenges regarding:

- Slip rings/brushes

  Likely to encounter problems like sparks, which make them a replaceable part over time [9, p.5]

  Brushless DFIG generators avoid this, but suffers more from low efficiency and larger machine sizes (more complex to construct) [9, p.5]

- Gearboxes

  Maintenance is required, which makes it a cost-oriented problem [20, p.3]

- Additional protection systems

  Directly grid connected stator makes the system vulnerable to voltage dips and other perturbations[20, p.3]

The PMSG system avoids most of the maintenance issues above (depending on which PMSG topology), making them more suitable to be placed in areas which are difficult to reach, offshore installations for example. Some articles even suggest that annual service costs for DFIG systems (Including service cost of the gearbox) could be 20-30% higher than service costs of PMSG [9, p.3].

In the case with medium and high-speed PMSGs(which requires gearbox), the service cost will undoubtedly increase, and it will add as a disadvantage similar to that of DFIG.

Maintenance costs regarding PMSG:

- Demagnitization of the magnets [20, p.5]
- Regular maintenance for gearboxes if MS and HS PMSG system is used

8.5 Summary table

Table 7 include research from previous Chapters in this thesis and summarizes some of the essential properties of both the DFIG and PMSG systems.

Properties of each system		
Configuration	**DFIG**	**PMSG (LS/DD,MS and HS)**
Generator Type	**Asynchronous**	**Synchronous**
Gearbox	**Yes** • Heat dissipation from friction • Needs regular maintenance • Adds more audiable noise	**No/Yes** • Not needed for low-speed applications (LS PMSG) • Needs gearbox for medium and high-speed applications
Generator	• DFIG allows for a higher output power production than what is rated, without overheating • Stator directly coupled to grid, making the system vulnerable to grid faults • The rotor can either consume or deliver power (sub- or hypersynchronous mode) • Has a limited variable speed range (±30% of synchronous speed) • Either excitation through brushes/slip rings or brushless configurations	• No need for external excitation current • Use of permanent magnets • Risk of demagnetization of the magnets at higher temperatures • If DD PMSG, more pole pairs are required (low speed) • Does not require slip rings
Converter	**Partial Converter** • Rating of the converter is between 25-30% of total power • The converter can inject reactive power to the grid and ensure smoother grid integration	**Full Converter** • Fully rated power converters (sized according to maximum power production) • Contributes even more to voltage re-establishment, by injecting a more considerable amount of reactive power to the grid during faults (due to converter size)

Properties of each system		
Efficiency	• High energy yield and efficiency • Total efficiency is affected by the gearbox, bearing, windage, stator, rotor, stray load, and converter losses • Lower efficiencies for brushless configurations(BDFIM).	• High energy yield and efficiency • Total efficiency is affected by the gearbox (only if HS or MS), bearing, windage, copper, stray load, and converter loss • Lower copper losses than DFIG
Maintenance	**Maintenance is required due to**: • Gearbox (Gear and bearing faults reduces longevity) • Brushes/slip rings (regularly controlled and replaced)	**Maintenance is required due to**: • Demagnitization of magnets • Gearbox (if MS and HS)
Cost	• The initial is lower cost for DFIG • Maintenance cost is higher for DFIG	• The initial cost is higher for PMSG • DD PMSG has lower maintenance cost compared to DFIG
Operating conditions	• More vulnerable to grid faults • More dependent on protection systems regarding grid related faults	• The converters "isolate" the generator from grid related faults • More robust against perturbations in the grid
Onshore/Offshore	• Common in onshore sites, were access and maintenance is easier • Offshore solutions do exist	• DD PMSG is suitable for offshore applications (less maintenance) • Medium and high-speed PMSG's are suitable for onshore applications

Table 7: Summary table

8.6 Conclusion

This these aimed to acquire knowledge about the DFIG and PMSG configuration through theoretical analysis and the use of simulations in Simulink. In order to achieve this, research is based on studying scientific articles, Ph.D.'s, online lectures, and related literature books as well as a visit to Midtfjellet Vindpark.

Specific challenges have presented themselves during the time of this study. The idea was to make two simulations programs, one of DFIG and other of PMSG with the possibility of a lab setup. Eventually, a decision was made to focus on one configuration in Simulink and take a more theoretical approach to the other due to the time estimated to achieve this.

Wind energy technologies up to this date keep developing in terms of efficiency, operational conditions, and cost-effectiveness. When evaluating the properties of each configuration through table 7, it can be seen that choosing a wind generator system is a subject to several considerations. Concluding with one configuration over the other proves challenging, especially when certain information as geographical locations and economic investment are unknown.

Both configurations have their pros and cons, but utilizing them correctly in the right environment is one key factor for deciding this. Another essential thing to consider is how much one is willing to invest in such a project. As for the case with DFIG, its initial cost is in general lower than PMSG.

When considering the installation of wind energy offshore most studies points towards the permanent magnet synchronous generator. Even though the initial cost is higher it is the better alternative due to lower maintenance costs. No brushes/slip rings are needed, and if it is direct driven, the gearbox can also be excluded. Transporting larger gearboxes can prove to be a challenge at sea. Also, it applies when removing old equipment and installing new. The PMSG efficiency from earlier studies and company datasheets prove to be high compared to other technologies. It also proves to be very reliable during grid faults, making operating conditions better. Minimum requirement of maintenance is preferable for offshore wind energy, and the DD PMSG has proven most suitable for this.

As for onshore installations, both DFIG and PMSG qualify. An advantage of DFIG, as previously mentioned, is the lower initial cost. If maintenance proves easy and accessible, the doubly-fed induction generator is an excellent alternative to choose. Even if grid faults should occur, they still prove reliable when installed with proper safety equipment (crowbar, and similar). With the ability to run with $\pm 30\%$ of synchronous speed makes it an excellent variable speed solution.

8.7 Future work

Some suggestions:

- Further studies of the PMSG
  - Simulink modeling
  - Grid fault analysis
  - Lab testing
- DFIG
  - Grid fault analysis
  - Lab testing
- BDFIG
  - Comprehensive study (including simulations)
  - Lab testing

References

[1] Abb dfig. https://search-ext.abb.com/library/Download.aspx?DocumentID=9AKK105233&LanguageCode=en&DocumentPartId=&Action=Launch. Accessed: 2019-05-03.

[2] Abb dfig. https://search-ext.abb.com/library/Download.aspx?DocumentID=3AUA0000231755&LanguageCode=en&DocumentPartId=&Action=Launch. Accessed: 2019-05-03.

[3] Abb dfig. https://new.abb.com/motors-generators/generators/generators-for-wind-turbines/doubly-fed-generators. Accessed: 2019-06-03.

[4] Abb hspmsg. https://search-ext.abb.com/library/Download.aspx?DocumentID=9AKK105293&LanguageCode=en&DocumentPartId=&Action=Launch. Accessed: 2019-05-24.

[5] Abb hspmsg. https://new.abb.com/motors-generators/generators/generators-for-wind-turbines/permanent-magnet-generators/high-speed-permanent-magnet-generators. Accessed: 2019-06-03.

[6] Abb lspmsg. https://new.abb.com/motors-generators/generators/generators-for-wind-turbines/permanent-magnet-generators/direct-drive-generators. Accessed: 2019-06-03.

[7] Abb mspmsg. https://search-ext.abb.com/library/Download.aspx?DocumentID=9AKK105541&LanguageCode=en&DocumentPartId=&Action=Launch. Accessed: 2019-05-24.

[8] Abb mspmsg. https://new.abb.com/motors-generators/generators/generators-for-wind-turbines/permanent-magnet-generators/medium-speed-permanent-magnet-generators. Accessed: 2019-06-03.

[9] Pmg vs. dfig – the big generator technology debate. https://theswitch.com/2014/03/20/pmg-vs-dfig-the-big-generator-technology-debate/. Accessed: 2019-04-30.

[10] Technical data midtfjellet vindpark. https://midtfjellet.no/om-oss/vindparken/. Accessed: 2019-04-29.

[11] Doubly fed induction machine : modeling and control for wind energy generation applications, 2011.

[12] Handbook of distributed generation : Electric power technologies, economics and environmental impacts, 2017.

[13] *IEEE Standard Test Procedure for Polyphase Induction Motors and Generators (112-2017)*. IEEE, New York, USA, 2018.

[14] Davide Aguglia, Philippe Viarouge, Rene Wamkeue, and Jerome Cros. Selection of gearbox ratio and power converters ratings for wind turbines equipped with doubly-fed induction generators. In *2007 IEEE International Electric Machines & Drives Conference*, volume 1, pages 447–452. IEEE, 2007.

[15] Davide Aguglia, Philippe Viarouge, René Wamkeue, and Jérôme Cros. Optimal selection of drive components for doubly-fed induction generator based wind turbines. In *Wind turbines*. IntechOpen, 2011.

[16] Argiñe Alacano, Juan José Valera, Gonzalo Abad, and Pedro Izurza. Power-electronic-based dc distribution systems for electrically propelled vessels: A multivariable modeling approach for design and analysis. *IEEE Journal of Emerging and Selected Topics in Power Electronics*, 5(4):1604–1620, 2017.

[17] Olimpo Anaya-Lara. Offshore wind energy generation : control, protection, and integration to electrical systems, 2014.

[18] D Bang, H Polinder, G Shrestha, and Jan Abraham Ferreira. Review of generator systems for direct-drive wind turbines. In *European wind energy conference & exhibition, Belgium*, volume 31, 2008.

[19] Anissia Beainy, Chantal Maatouk, Nazih Moubayed, and Fouad Kaddah. Comparison of different types of generator for wind energy conversion system topologies. In *2016 3rd International Conference on Renewable Energies for Developing Countries (REDEC)*, pages 1–6. IEEE, 2016.

[20] A Akhilesh Kumar Gupta B Himanshu and Bhushan C Paulson Samuel. Generator topologies with power electronics converters for a wind energy conversion system: A review. In *Proc. IEEE Int. Conf.*

[21] Ahmed A Hossam-Eldin, Karim H Youssef, and Kareem M AboRas. Wind power generation based on pmsg system using matlab simulink.

[22] Emma Aberg (International Renewable Energy Agency – IRENA), Rana Adib (REN21), Fabiani Appavou, Adam Brown, Scott Dwyer (ISF-UTS), Barbel Epp (solrico), Flávia Guerra (REN21), Bozhil Kondev, Hannah E. Murdock (REN21), Evan Musolino, Jay Rutovitz (ISF-UTS), Janet L. Sawin (Sunna Research), Kristin Seyboth (KMS Research, Consulting), Jonathan Skeen (SOLA Future Energy), Freyr Sverrisson (Sunna Research), Sven Teske (ISF-UTS), Stephanie Weckend (IRENA), and Henning Wuester (IRENA). Renewables 2018 global status report. *A comprehensive annual overview of the state of renewable energy*, 2018.

[23] NAVEED UR REHMAN MALIK. Modelling, analysis, and control aspects of a rotating power electronic brushless doubly-fed induction generator. 2015.

[24] Alexey Matveev. Novel pm generators for large wind turbines.

[25] Patrick A Narbel, Jan Petter Hansen, and Jan R Lien. *Energy technologies and economics*. Springer, 2014.

[26] DH Nguyen and M Negnevitsky. A review of fault ride through strategies for different wind turbine systems. In *2010 20th Australasian Universities Power Engineering Conference*, pages 1–5. IEEE, 2010.

[27] Andreas Petersson. *Analysis, modeling and control of doubly-fed induction generators for wind turbines*. Chalmers University of Technology, 2005.

[28] N.A. Prashanth and P Sujatha. Commonly used wind generator systems: A comparison note. *Indonesian Journal of Electrical Engineering and Computer Science*, 7:299–311, 08 2017.

[29] Dmitry Svechkarenko. *On design and analysis of a novel transverse flux generator for direct-driven wind application*. PhD thesis, KTH, 2010.

[30] Mehdi Taghizadeh Kakhki. Modeling of losses in a permanent magnet machine fed by a pwm supply. 2016.

[31] R Takahashi, H Ichita, J Tamura, M Kimura, M Ichinose, M Futami, and K Ide. Efficiency calculation of wind turbine generation system with doubly-fed induction generator. In *XIX International Conference on Electrical Machines - ICEM 2010*, pages 1–4. IEEE, 2010.

[32] Wildi Theodore et al. *Electrical machines, drives and power systems, 6/E*. Pearson Education India, 2007.

[33] Annual Market Update. Global wind report. *Global Wind Energy Council*, 2017.

[34] Jin Yang, John E Fletcher, and John O'Reilly. A series-dynamic-resistor-based converter protection scheme for doubly-fed induction generator during various fault conditions. *IEEE Transactions on Energy conversion*, 25(2):422–432, 2010.

Appendices

A Simulink model

A.1 How values from table 5 is calculated

A.1.1 Wind speed

The wind speed (v) works as a constant in Simulink. This value can be changed either directly in Simulink or the pre-defined values in Matlab worksheet.

A.1.2 Mechanical speed (Ω_m) and torque

Ω_m and the electromagnetic torque (Tem) is measured directly from the Simulink circuit. It is also represented in the Simulink scope to analyze any changes in the simulation.

A.1.3 Angular frequencies and slip

The angular frequencies are described in Chapter 5.1, and are calculated as follows:

Angular frequency of the voltages and currents in the stator windings:

$\omega_s = 2 * \pi * f$

Angular frequency of the voltages and currents in the rotor windings [11, p.157]:

$\omega_m = \Omega_m * p$

Angular frequency of the rotor[11, p.157]:

$\omega_r = \omega_s - \omega_m$

This results in the formula for slip (s)[11, p.157]:

$s = \frac{\omega_s - \omega_m}{\omega_s}$

A.1.4 Ideal power calculations

Pm_{NoLoss} represents the mechanical power produced by the wind turbine. When neglecting the gearbox losses, the mechanical power is transferred directly to the generator[11, p.157].

$Pm_{NoLoss} = \Omega_m * Tem = Tem * \frac{\omega_m}{p}$

The ideal stator and rotor power is calculated as[11, p.170-171]:

$Ps_{NoLoss} = Tem * \frac{\omega_s}{p}$

$Pr_{NoLoss} = -Ps_{NoLoss} * (s)$

A.1.5 Power losses

The gearbox efficiency calculation:

$Efficency_{Gearbox} = \frac{Pm_{NoLoss} - P_{mR} * 0.01 * q}{Pm_{NoLoss}}$

Where:

- PmR is the rated Wind turbine power
- 0.01 is the viscous loss proportion of 1%
- q number of gearbox stages (In this case set to 3)

The actual loss is found subtracting power before and after the gearbox:

$P_{GearboxLoss} = Pm_{NoLoss} - P$

P is the power after gearbox loss is subtracted. This value is also used to find the stray load loss:

$P_{StrayLoss} = 0.005 * \frac{P^2}{P_{RatedStatorPower}}$

This results in a mechanical power to the generator as follows:

$P_{Mech} = Pm_{NoLoss} - P_{GearboxLoss} - P_{StrayLoss}$

A.1.6 Stator current and Cu-Loss

The stator power without Cu-loss is given by:

$Ps = \frac{P_{Mech}}{1 - Slip}$

The calculation of the stator current:

$Is = \frac{Ps}{Vs * \sqrt{3}}$

The total Cu-loss calculation in the stator circuit:

$Ps_{CuLoss} = (Is)^2 * Rs * 3$

A.1.7 Rotor current and Cu-Loss

The rotor power without Cu-loss is given by:

$Pr = \frac{-P_{Mech}}{1-Slip}$

The rotor current is calculated similarly to the stator. The calculation refers I_r to the grid side voltage:

$Ir = \frac{Pr}{Vs*\sqrt{3}}$

The total Cu-loss in the rotor circuit can be calculated, with the rotor side resistance R_r referred to the stator side:

$Pr_{CuLoss} = (Ir)^2 * Rr * 3$

The rotor side losses also include the power lost in the converter. The efficiency of converters are usually high (Approx. 97%). 3% loss is assumed:

$Pr_{ConverterLoss} = Pr * 0.03$

A.1.8 Stator and rotor power with losses

Ps is power delivered to the grid. It means that Cu-loss is positive oriented, while Ps is negative. It is why the formula has a positive sign for the Cu-loss.

$Ps_{WithLoss} = Ps + Ps_{CuLoss}$

The rotor side power flow in DFIG is either positive or negative oriented. It depends if the generator runs in sub-or hypersynchronous mode. The result is that the losses either is subtracted or added:

$Pr_{WithLosses} = Pr \pm Pr_{CuLoss} \pm Pr_{ConverterLoss}$

A.1.9 Power delivered, efficiency and C_P

The calculation of total power delivered to the grid:

$P_{Total} = Ps_{WithLoss} + Pr_{WithLosses}$

The total efficiency:

$Efficiency = \frac{P_{Total}}{Pm_{NoLoss}}$

And finally the C_P:

$C_P = \frac{Pm_{NoLoss}}{\frac{1}{2}*\rho*\pi*R^2*v^3}$

B ABB generator datasheets and figures

B.1 High-speed PMSG

Typical performance characteristics of the AMG 500 and 560 series:	
Power	1.5 to 3.6 MW
Efficiency at rated speed	98% (at 20% load > 97%)
Cooling	air or water cooling
Mounting and protection	IM1001 (inclined 4...6 deg), IP54
Voltage	690 V +/-10 %, 50 or 60 Hz Medium voltage (i.e. 4 kV)
Rated speed options	from 1000 to 1800 rpm
Operation speed range	0...2000 rpm
Max. overspeed	up to 3000 rpm
Insulation class/Temp. rise	F / B
Ambient temperature range	-20°C ... +40°C; extended -30°C ... +50°C
Typical dimensions, weight	500: L2500 x W1700 x H1800, 5–7 tn 560: L3000 x W2100 x H1900, 7–10 tn

Figure 47: ABB high-speed PMSG datasheet[4]

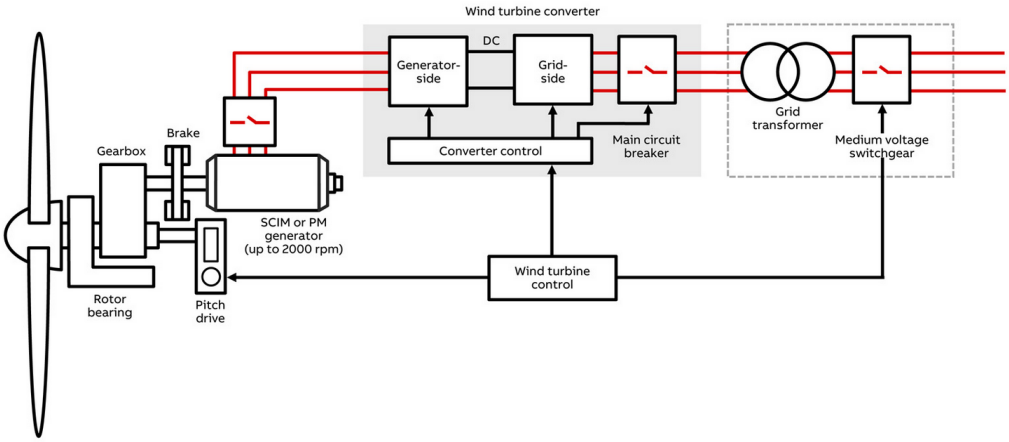

Figure 48: High-speed PMSG[5]

B.2 Medium-speed PMSG

Typical data for medium speed generators up to 8 MW:	
Frame size	710 - 1120
Power	1 - 8 MW
Nominal speed	between 100 - 500 rpm
Efficiency	Over 98 % (also at 20 % load)
Cooling	Typically water cooled
Voltage	690 - 3300 V or higher
Frequency	50 and 60 Hz
Ambient	Standard: - 20°C ... +50°C Low temp: - 30°C ... +50°C
Typical dimensions in 500 rpm design (LxWxH, weight)	3 MW: 2400 x 1800 x 2000 ; ~ 12.5 tn 5 MW: 2900 x 3000 x 3350 ; ~ 18.2 tn 7 MW: 2900 x 3300 x 3600 ; ~ 24.9 tn

Figure 49: ABB medium-speed PMSG datasheet[7]

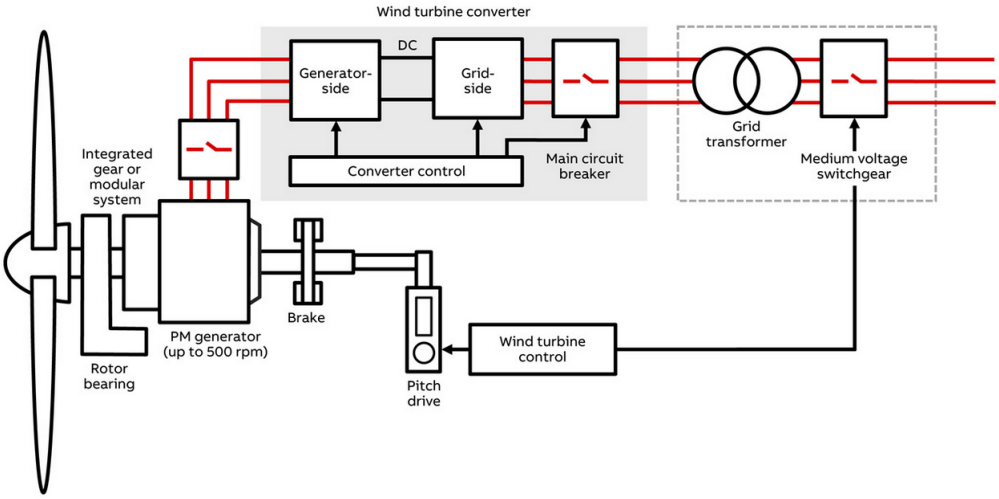

Figure 50: Medium-speed PMSG[8]

B.3 Low-speed PMSG

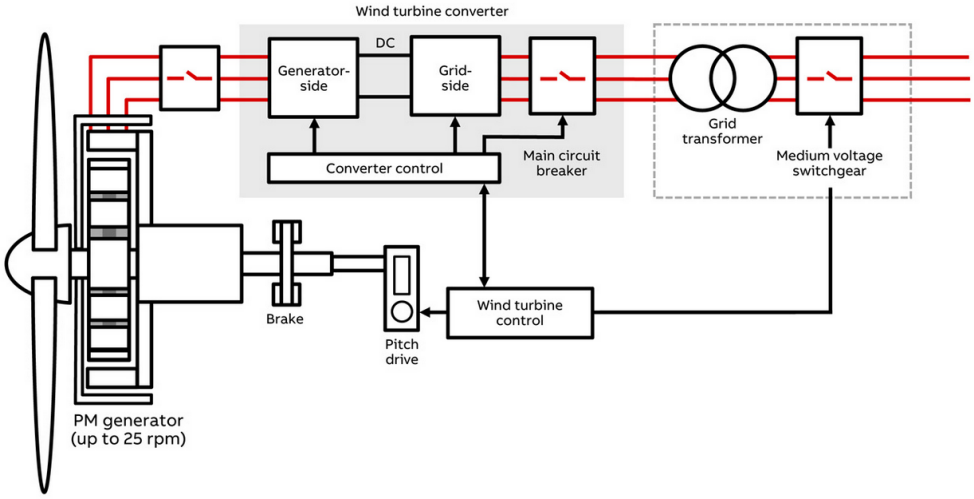

Figure 51: Low-speed(DD) PMSG[6]

B.4 DFIG

Typical data of the AMK/L series < 3.6 MW:	
Frame/power	500: up to 2.2 MW 560: up to 3.2 MW 630: up to 3.6 MW
Efficiency at rated speed	appr. 97...97.5%
Cooling (air or water)	IC 616/666, IC81/86W, SRU IC01/06
Mounting and protection	IM1001 (inclined 4...8 deg), IP54, SRU IP23
Voltage	690–1000 V +/-10%, 50 or 60 Hz 3–6 kV +/-10%, 50 or 60 Hz (630 frame)
Locked rotor voltage	approx. 1800 V or 2000 V
Rated speed (typical)	1750 rpm, 1200 rpm (50 Hz) 2100 rpm, 1440 rpm (60 Hz)
Operation speed range	1000...2000 rpm/670...1330 rpm (50 Hz) 1200...2400 rpm/800...1600 rpm (60 Hz)
Max. overspeed	3000/2300 rpm depending on size
Power factor	p.f. 0.90 cap ...1.0 ... 0.90 ind
Insulation class/Temp. rise	F/B (at Un, p.f. 0.95 cap and 40°C), or F/F
Temperature range	-20°C...+40°C; extended -30°C...+50°C
Dimensions and weight (depending on power)	500: L3150 x W1600 x H1850 mm, 6–6.7 tn 560: L3300 x W1650 x H2050 mm, 7–10 tn 630: L3500 x W1700 x H2250 mm, 9–12 tn

Figure 52: ABB DFIG datasheet[1]

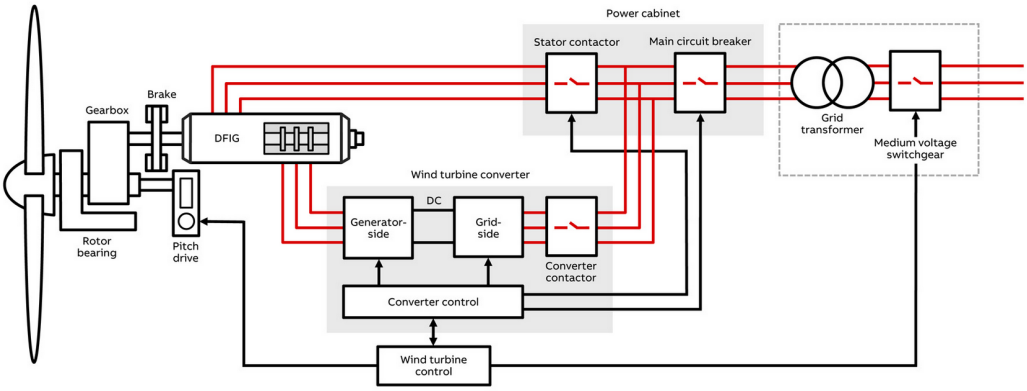

Figure 53: ABB DFIG[3]

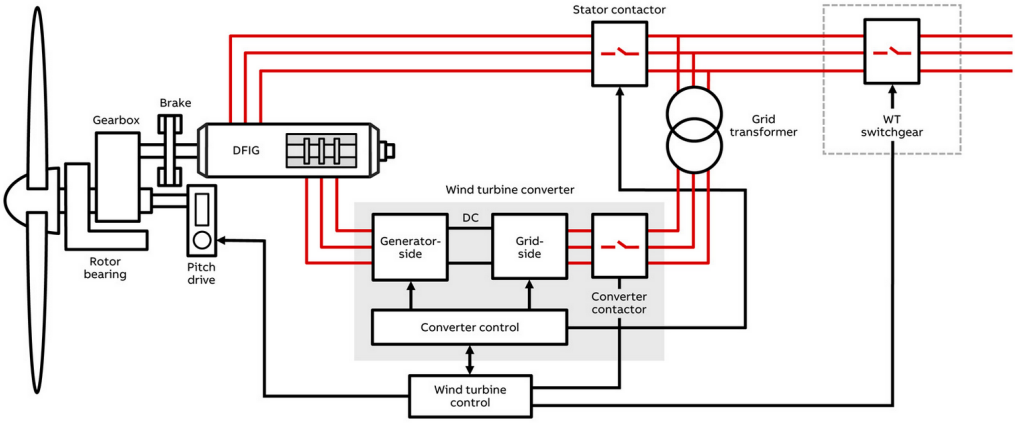

Figure 54: ABB DFIG[3]

C Midtfjellet Vindpark

During this thesis, I made contact with Midtfjellet Vindpark and applied on their webpage to visit one of their wind turbines. They quickly responded, and we made arrangements for a tour in their wind park.

C.1 Technical data about Midtfjellet Vindpark

Midtfjellet Vindpark	
Yearly Production	433.7GWh
Amount of windturbines type N90, 2500KW	34
Amount of windturbines type N100, 2500KW	10
Amount of windturbines type N117, 3600KW	11
Lenght of high voltage cables	150km
Switchgear	34kV
Main transformer (Phase 3)	300/66/34kV, 100MW
Switchgear	300kV
High voltage line to Børtveit	10km 300kV, 800MVA
Roads	About 30km
Foundation/Reinforcement	$107m^3$ concrete / 18 tonns reinforcement per turbine

Table 8: About Midtfjellet Vindpark [10]

- Phase 1 was set in operation 01.06.2013, with 21 turbines[10]
- Phase 2 was set in operation 01.12.2013, with 23 turbines[10]
- Phase 3 was put in commercial operation 10.08.2013 with 11 turbines, which gives a total amount of 55 turbines[10]

More information about how the construction process, during phase 1,2 and 3, of the wind park can be found at their homepage [10]

C.2 My visit

After signing the necessary precaution papers and being formally introduced to the staff. They explained that taking pictures is allowed outside of the wind turbine. Taking pictures inside the turbine was prohibited. Here are some of the pictures from the expedition:

Figure 55: Midtfjellet Vindpark

Figure 56: Midtfjellet Vindpark

Figure 57: Midtfjellet Vindpark

Figure 58: Midtfjellet Vindpark

Figure 59: Midtfjellet Vindpark